LBNL-47939
LAUR 01-2574
CBP tech note 230
11/2000

700 MHz Window R&D at LBNL

R. Rimmer, G. Koehler, T. Saleh, R. Weidenbach

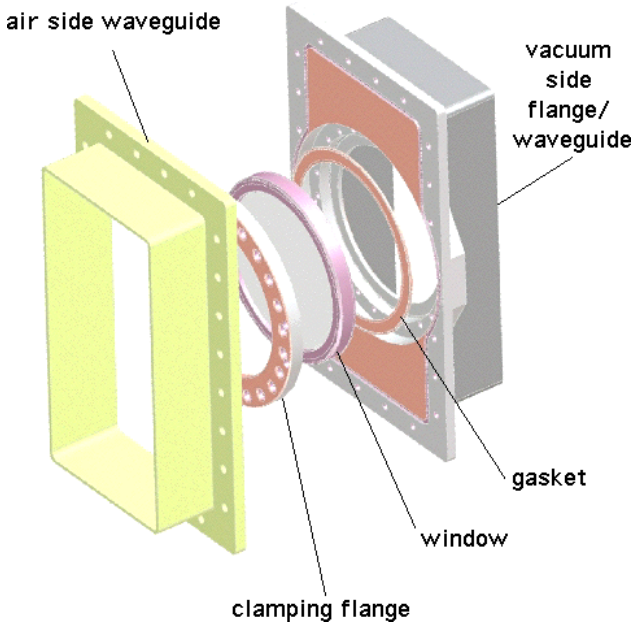

Abstract

This document describes the R&D activities at LBNL under contract # 06261-001-99 2A "700 MHz RF Window" from LANL. The Conceptual design, numerical modelling, cold-testing, and manufacturing steps are described. Recommendations for assembly and testing proceedures are included. Some possible future developments are discussed. A drawing package and cost estimate for volume production are also included.

This project has produced four high-power prototype windows and established a manufacturing process that could be transferred to industry should large scale production be required. It is hoped that this design will be useful for the LEDA test program and for future projects. The same design with slight modifications is intended to be used for the Linear Collider damping ring RF cavities at 714 MHz. Funding, facilities and personnel from that study augmented those from LANL.

The four prototype windows will be high-power tested at LANL. Results of the high power tests will be published separately.

Contents

Introduction

LEDA requires RF windows with a high average power throughput and reliable operation. It is proposed to use a scaled version of the PEP-II disk RF window [1], which is designed to be robust and withstand high power throughput continuously. Figure 1 shows the proposed window assembly.

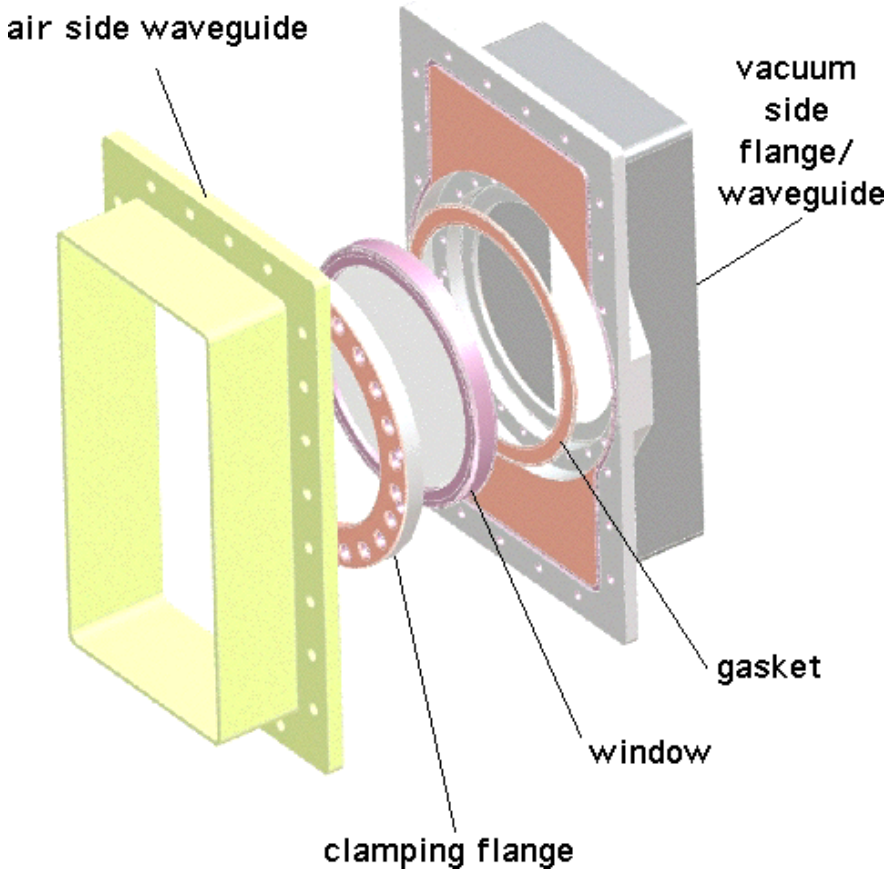

Figure 1. waveguide window assembly.

The waveguide chosen for the LEDA RF system is WR1500. For simplicity it is proposed to use the same waveguide size for both the air side and vacuum side of the window, which requires some adjustment of the dimensions from the PEP-II design.

The window fabrication follows the same process developed for PEP-II, resulting in rugged design with the ceramic pre-stressed in compression by a strong stainless steel ring, which also contains the cooling channel. This pre-stress is designed to compensate the tensile stresses that would otherwise be induced in the ceramic due to heating by RF losses.

1. Window analysis in MAFIA

The window design has been studied using MAFIA, employing the time domain module T3 with the S-parameter macro which can calculate steady state reflection and transmission coefficients, VSWR etc. These can be calculated on a frequency by frequency basis or with a broad-band approximation using a pulse excitation. Because of the inherent symmetry in the design only a quarter of the geometry need be modeled. Figure 2 shows the MAFIA model used for the studies. A finer mesh was also run to verify the accuracy of the results for a few cases. The geometry was defined by a few parameters; the waveguide height and width, the iris thickness, the window diameter and the ceramic thickness. All of these factors influence the match frequency to various extents, as does the dielectric constant of the ceramic, which was assumed to be 9.6 for these simulations. The match frequency is most sensitive to the diameter of the window and the ceramic thickness and less so to the iris thickness. For the lowest stress it is desirable to use the largest diameter window that will fit within the waveguide, while the dimensions of the stainless ring around the ceramic were scaled in proportion to keep the same aspect ratio as the successful PEP-II design. A size was chosen that neatly fits in the waveguide and allows a standard (10") circular "Conflat" knife edge geometry to be used. Once the diameter of the ceramic is chosen the frequency can be tuned by adjusting the thickness. This design has been chosen to allow the frequency to be set at 700 MHz for LEDA, figure 3. The final ceramic thickness was determined by measurements of actual ceramics in a cold-test fixture.

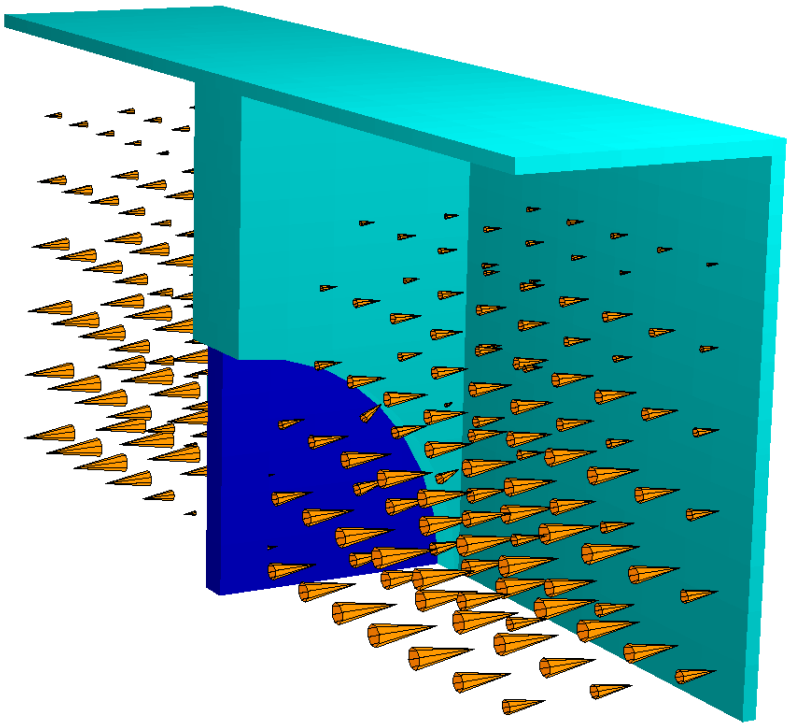

Figure 2 Window with normal TM_{01} waveguide mode propagating.

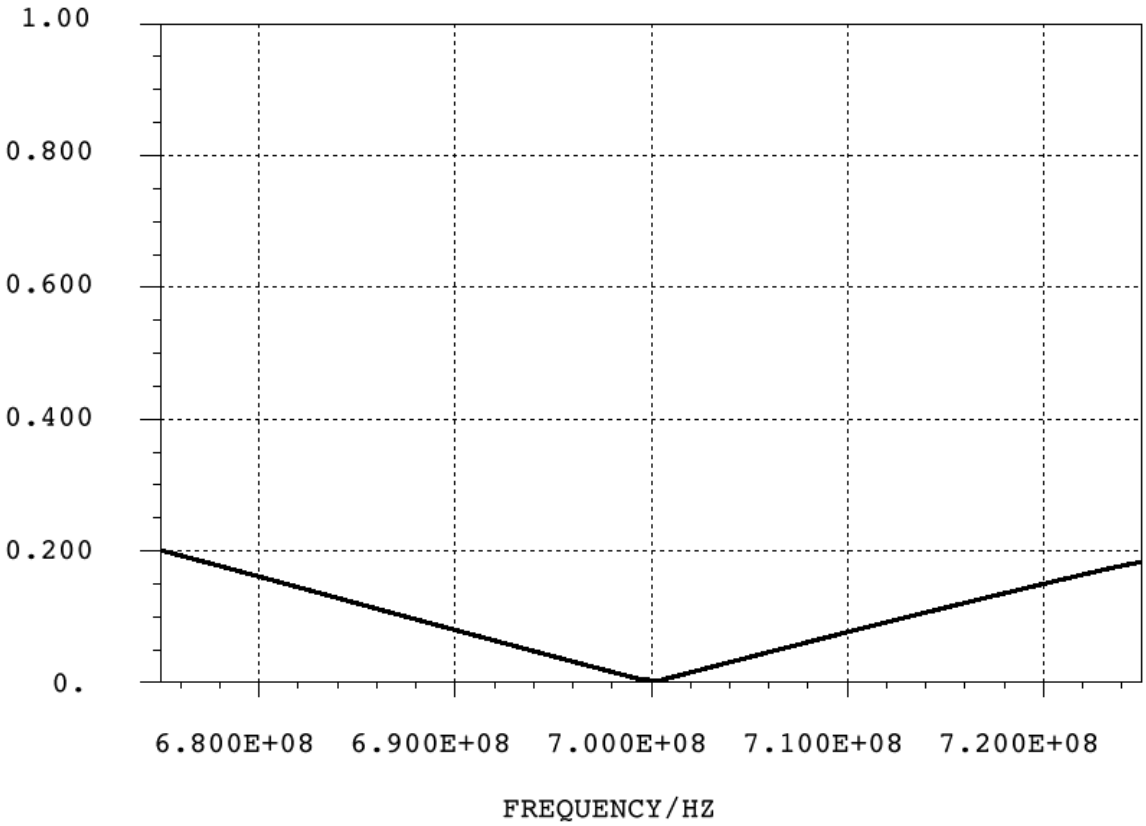

Figure 3. S_{11} of waveguide window.

Figure 4 shows how the frequency varies with ceramic thickness and iris length for the chosen geometry. To allow for manufacturing tolerances the window match frequency can be fine tuned by trimming the thickness of the flange when the knife edge is cut, the last step of the manufacturing sequence. Brazed assemblies were made slightly oversize on the flange thickness to allow them to be cut to final size after the frequency is measured in the cold-test fixture.

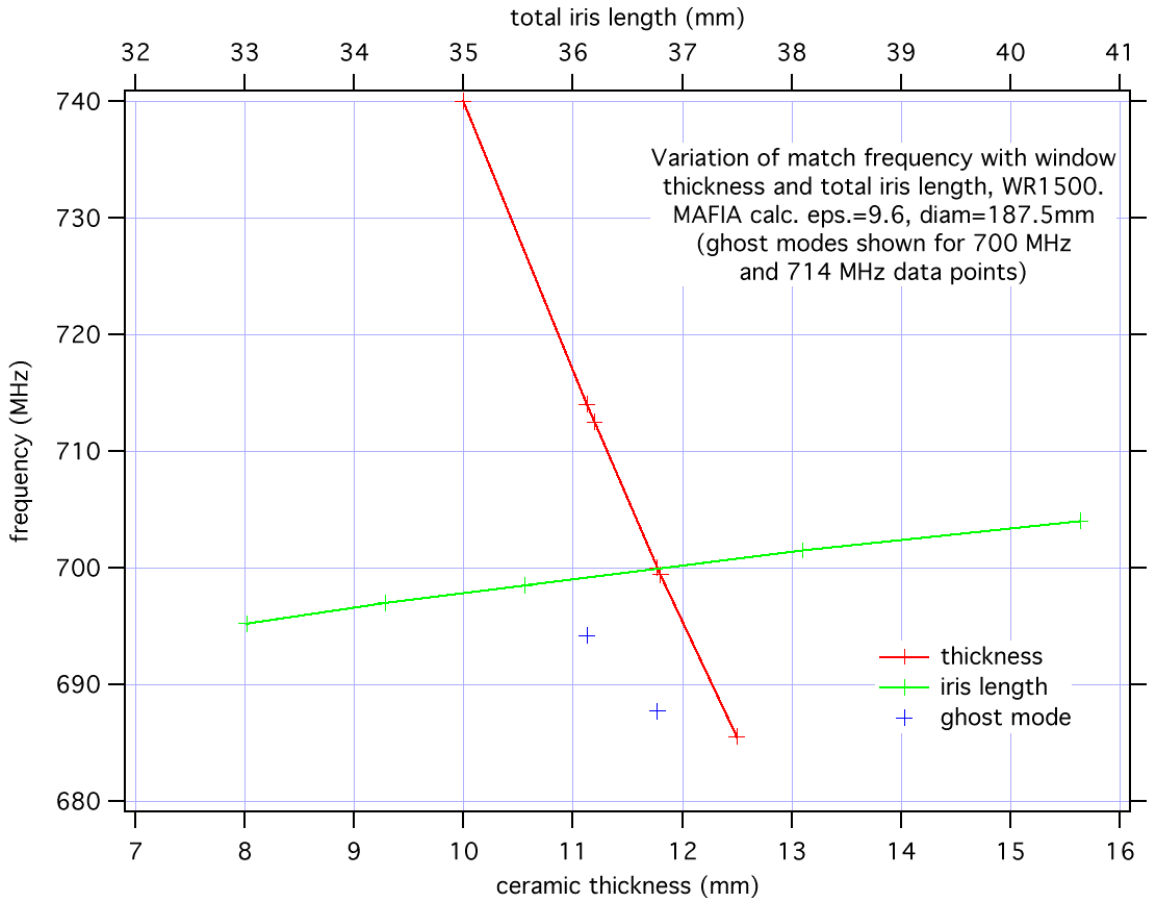

Figure 4. Tuning of window assembly.

The ceramic disk window in a waveguide can be thought of as a capacitively loaded iris in which the magnitude of the capacitive reactance equals that of the inductive part at the match frequency. This geometry can have other resonant modes, including the so-called "ghost mode" in which the electric and magnetic fields are orthogonal to the transmission mode and consequently are not able to propagate away in the waveguide. Figure 5 shows the electric field

distribution of the ghost mode in the window calculated by a frequency domain simulation in MAFIA. It is important that the waveguides in the MAFIA model be long enough that the waveguide termination does not influence the ghost mode frequency, so the model was run with increasingly long waveguides until the resonant frequency did not change significantly (1m long waveguides proved sufficient). It is important to make sure that the ghost mode is outside of the operating band of the RF system, otherwise power from the klystron or beam-induced power from the cavities could excite this mode causing heating of the ceramic. Figure 4 shows the ghost mode frequency for the 700 MHz geometry, which is safely outside of the operating band.

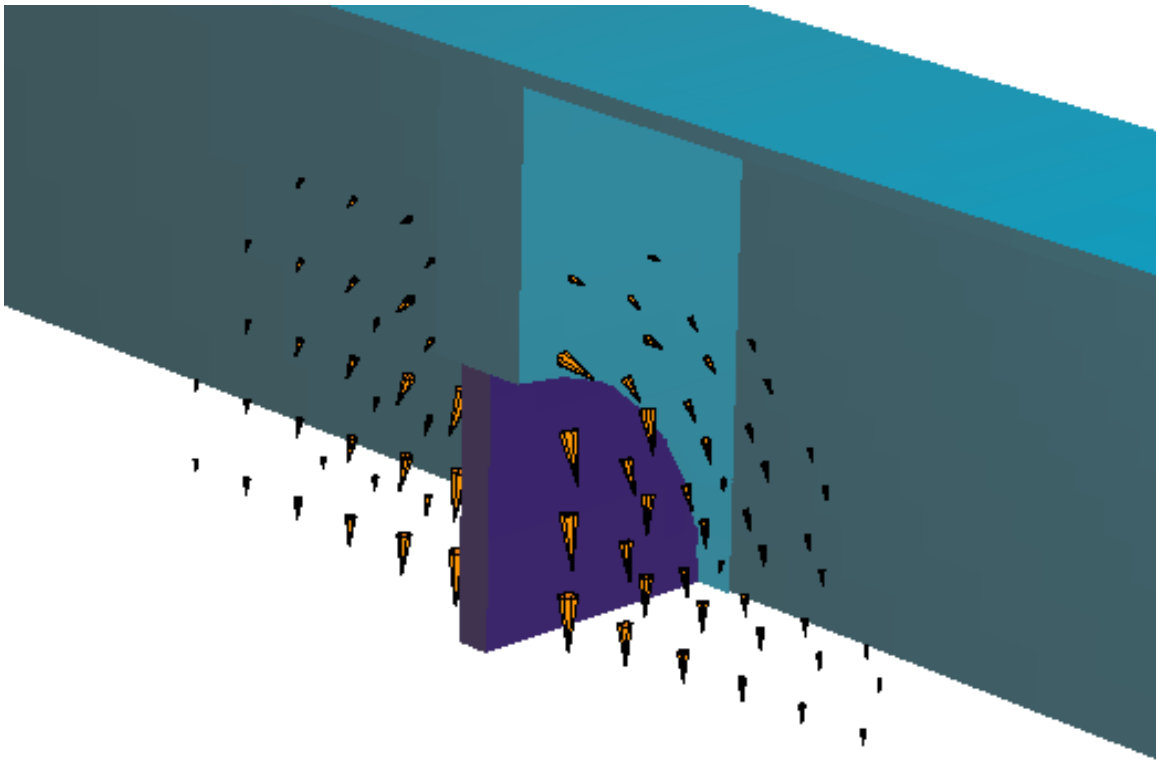

Figure 5. Electric field of ghost mode in window.

2. Cold-test measurements

In order to specify the thickness of the windows for production the dimensions of the ceramic were fine tuned by RF measurements in a cold-test model of the iris, figure 6. Two ceramics were initially ordered, one at the thickness estimated from the MAFIA runs and

one a little thicker. The two ceramics were measured in a simple fixture and the frequencies compared with the MAFIA predictions. Figure 7 shows the calculated and measured match frequency verses ceramic thickness. There is a small offset between the two curves, which can be accounted for by the actual dielectric constant being slightly different from that assumed in the MAFIA calculations. The slope of the curve predicted by MAFIA is -19.9 MHz/mm, while that from the measurements is -19.5 MHz/mm. The slope of the measured data was used to extrapolate to estimate the ceramic thickness which should yield a match frequency of 700 MHz. Note that there is a second slight offset in the plots because the simple fixture was slightly thicker than the final flange thickness. This was accounted for in the tuning and the ground ceramic when remeasured came out very close to the expected frequency (701.1875 measured vs 700.537 expected). Figures 8,9 show the measured Transmission and reflection coefficients for the tuned window in the simple test fixture. Figure 10 shows the reflection coefficient on a linear scale to compare with figure 3. When the ground ceramic was measured in a new fixture with the correct thickness the frequency dropped to 699.6875, which is within the measurement accuracy of the desired value.

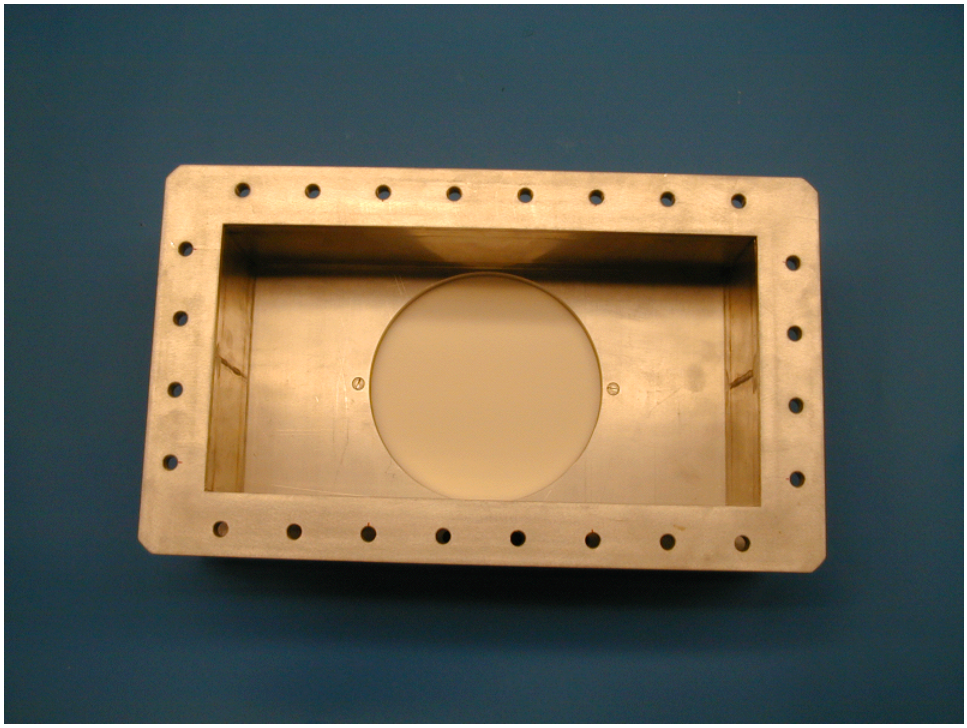

Figure 6. Simple cold test fixture.

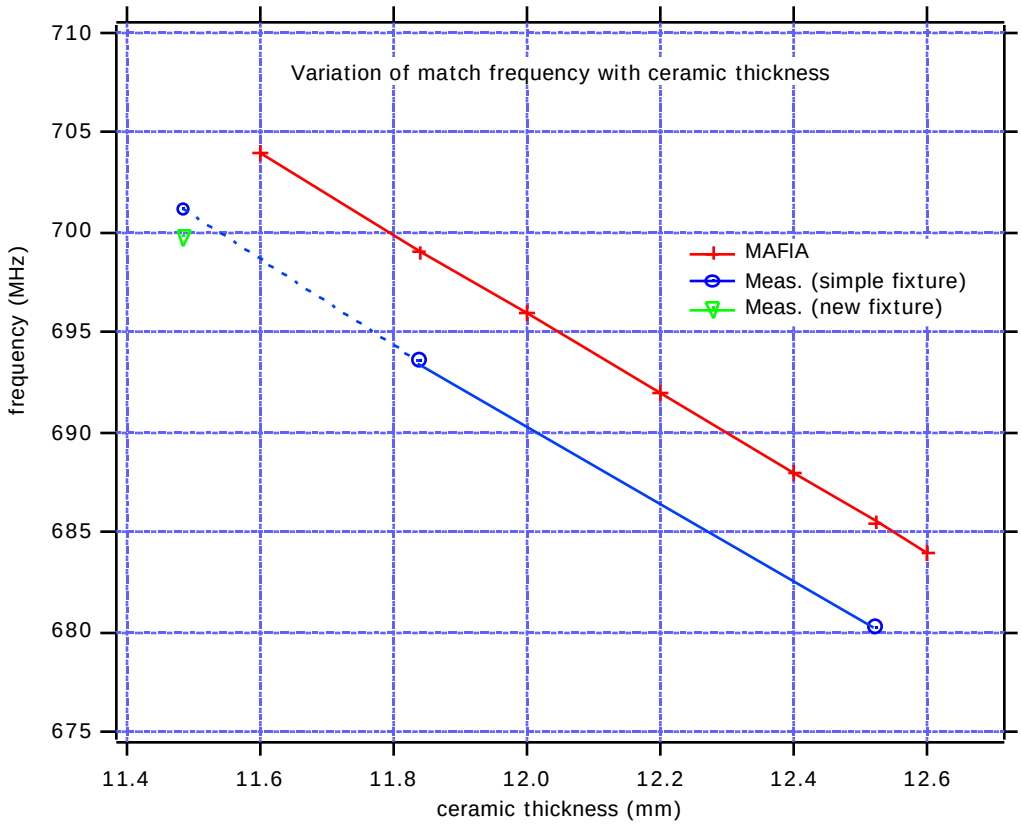

Figure 7. Variation of match frequency with ceramic thickness.

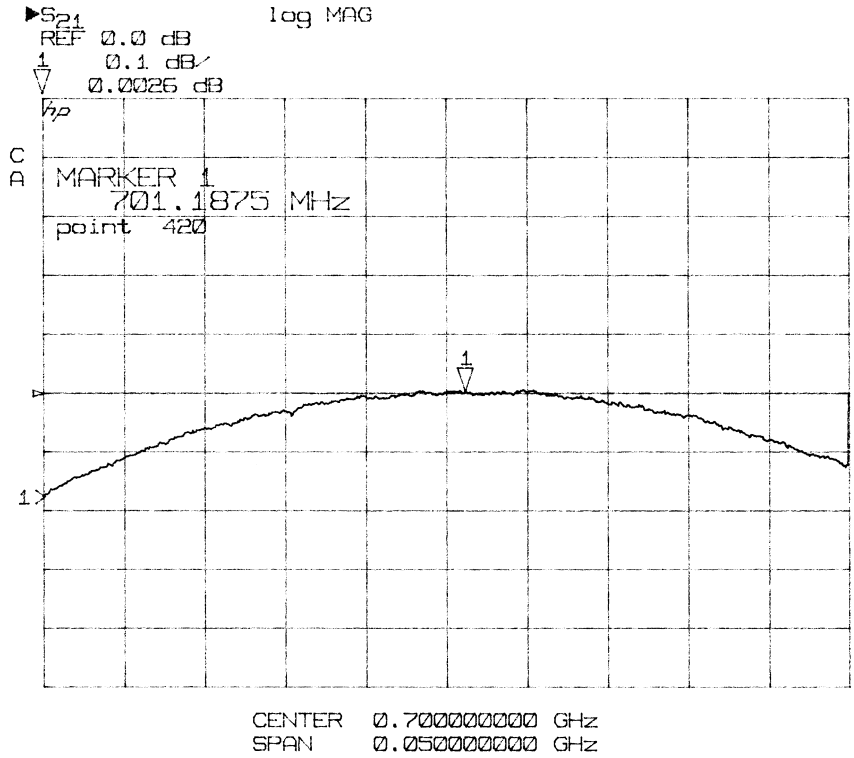

Figure 8. S_{21} of tuned ceramic in simple cold-test fixture.

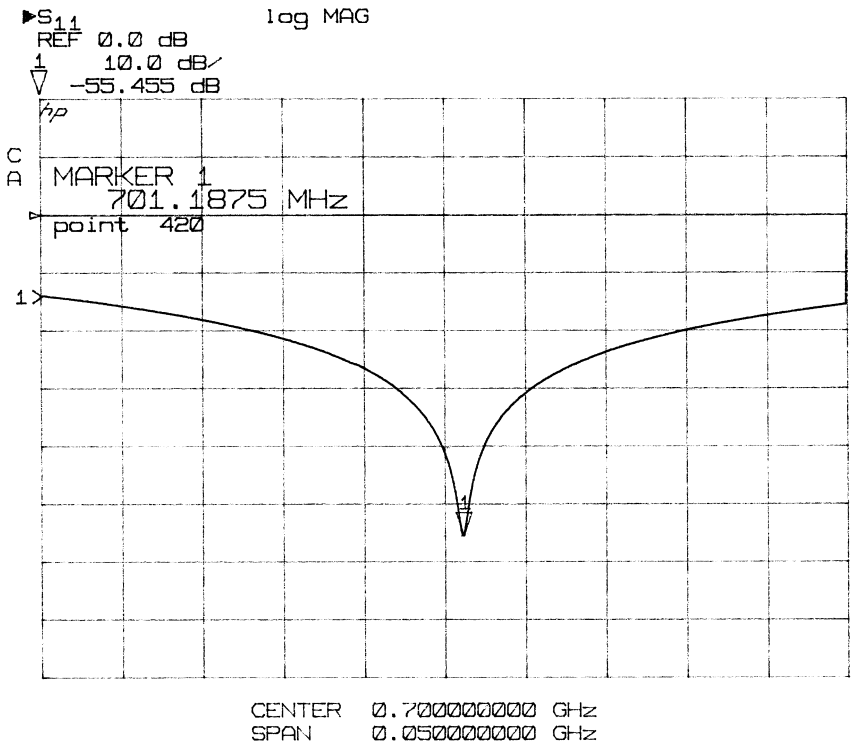

Figure 9 S_{11} of tuned ceramic in simple cold-test fixture.

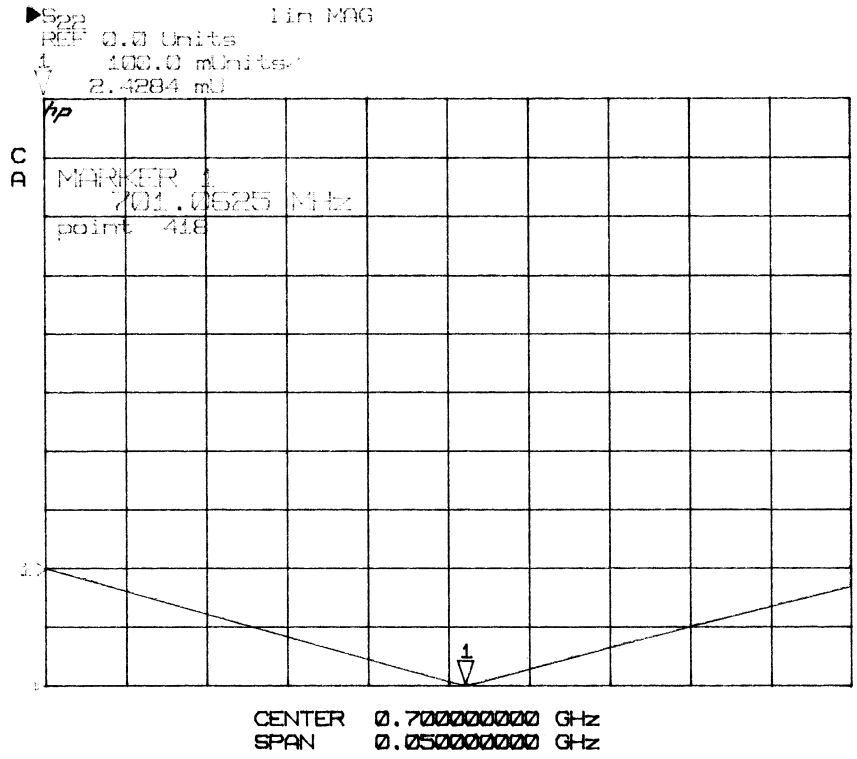

Figure 10. S_{11} of tuned ceramic, linear scale.

3. Window analysis in ANSYS

In service this window could see a temperature rise of up to 70°C due to RF losses in the ceramic and coating, multipactoring etc., which could cause the window to crack under thermal expansion. In order to solve this problem for the PEP-II B-Factory, a procedure was developed for creating a vacuum tight alumina window that is under compression under all operating conditions [2].

The method involves brazing the alumina window to a stainless steel cooling ring at high temperature. Since a small gap is required at the brazing temperature to promote braze flowing by capillary action, and the stainless steel has a higher coefficient of thermal expansion (CTE) than alumina, the stainless steel ring will contract more than the ceramic during cooling and place the alumina disk under compression. Conventionally this same difference in CTE would necessitate starting with a stainless steel ring which is smaller than the alumina window at room temperature. This would make assembly in the brazing furnace difficult.

The solution is to begin with a stainless steel ring which is slightly larger than the alumina window at room temperature, and can therefore be placed around the ceramic. A substantial molybdenum keeper ring is then placed around the stainless steel ring, again with a small clearance at room temperature. As the assembly is heated in the furnace, the stainless steel expands faster than the alumina and the molybdenum, which has the lowest CTE of the three. The stainless steel contacts the molybdenum ring which resists its expansion. As the temperature increases the stainless steel plastically deforms and is kept from expanding as much as it would otherwise. As the temperature continues to rise the alumina ring catches up to the stainless steel ring/molybdenum combination, until the desired brazing gap is attained at brazing temperature.

The molybdenum keeper ring is coated with TiN to reduce friction between it and the stainless steel ring. The stainless steel ring is "greened" (coated with Cr_2O_3), in a furnace to keep it from sticking to the molybdenum (in later brazes a greened shim was used between the cooling ring and the molybdenum keeper to further reduce the chances of sticking) The inner diameter of the stainless steel is coated with a 0.040” layer of copper to act as a stress relieving "buffer" layer between it and the alumina on the cooling cycle.

On cool down from the braze temperature the stainless steel ring contracts more than the Alumina creating the desired compressive pre-stress in the ceramic.

The key to this operation is starting with the correct initial clearances and sizes of the stainless steel and molybdenum rings. The size of the alumina window is determined by the RF frequency and the waveguide dimensions. For the PEP-II window an ANSYS FEA model was used and numerous experiments were performed to find the correct clearances and sizes for the molybdenum and the stainless steel rings. The PEP-II window was approximately 1.3 times the diameter of the new window, however the stainless steel ring size and the initial clearances do not scale exactly with the window and must be reevaluated.

In order to adapt the design for 700 MHz, the alumina was sized appropriately for the RF requirements and the molybdenum keeper ring was roughly sized by scaling the PEP-II ring. Using these inputs another ANSYS model was generated and the correct initial size and clearances were determined. The ANSYS model was experimentally checked by running a stainless steel and molybdenum ring of the predicted size through a furnace cycle before the first window braze is attempted. Using the results of this ring test the parameters of the ANSYS model were fine tuned and the final dimensions for the rings and the room temperature clearances will be determined. One complication arose in that the inner diameter of the keeper ring changed during the tests, see section 4, which was not expected from the predicted stress levels in the molybdenum. This may have been due to densification of the material in the interface area which was in the middle of the plate and may not have been fully densified during the plate rolling at the mill (The Molybdenum plate was originally made by a powder mettalurgy process). These changes required the dimensions of the cooling rings to be made different for each braze test in order to maintain the optimal clearances.

Initially, room temperature clearances of approximately 0.010” between the alumina and stainless steel and 0.015” between the stainless steel and molybdenum were used. The ANSYS model was built using 2-D axisymmetric elements. Figure 11 shows a radial slice of the assembly with the alumina window, the copper layer, the stainless steel and the molybdenum.

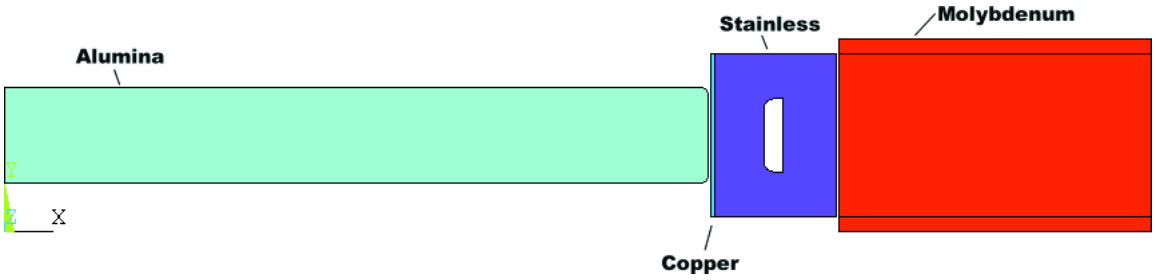

Figure 11. Material configuration for 700 MHz window braze.

Figure 12 shows a close up of the stainless steel cross section at room temperature. The gaps between the alumina and stainless and the stainless and molybdenum can be seen clearly. Contact elements are used in the ANSYS model in the gap between the stainless and the molybdenum to model the friction and sliding between the rings. Figure 13 shows the assembly at the brazing temperature of 1050°C. The 0.003" brazing gap between the stainless steel ring and the alumina window is barely distinguishable at this resolution. Figure 14 shows the Von Mises stress state in the stainless steel ring at brazing temperature. Note the stresses shown (in MPa) are uniformly above 96.6 MPa, the yield point of 316 stainless steel at elevated temperature.

Once the braze is made the temperature is ramped down slowly and the stainless contracts around the ceramic. There is a long hold at constant temperature part way through the cool down which is to allow the copper buffer layer to creep, relieving some of the stresses caused by the axial differential contraction. On cooling to room temperature the stainless steel is in tension and the ceramic is pre-stressed in compression.

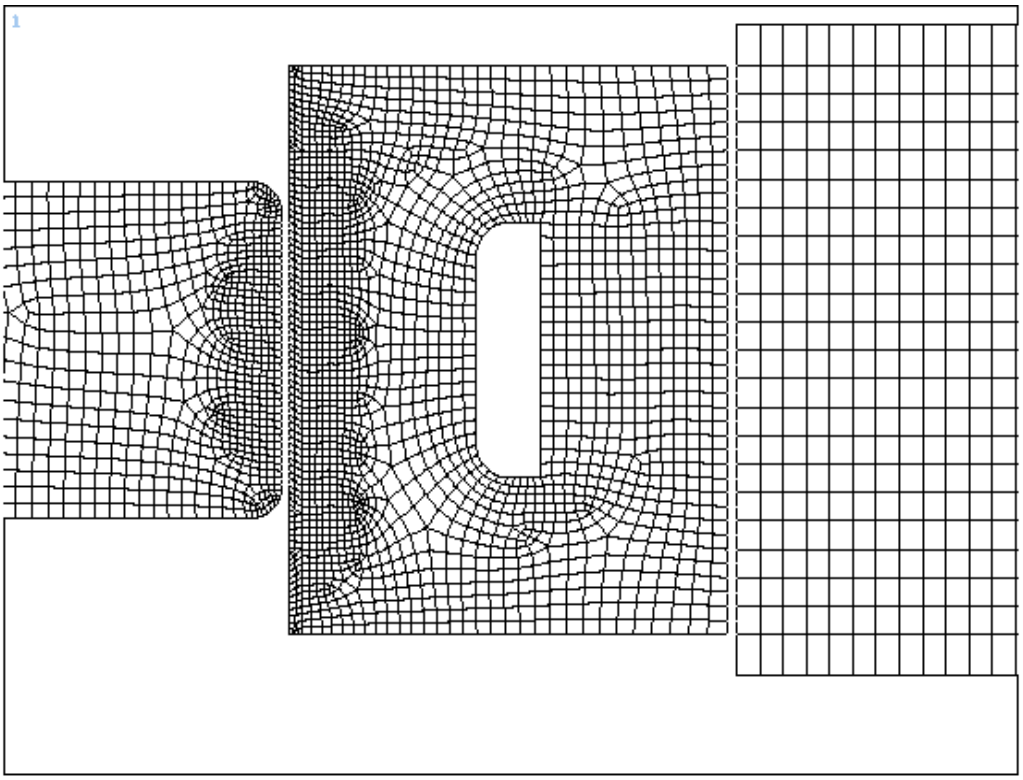

Figure 12. ANSYS model showing FE mesh and clearances between the materials at the start of the cycle.

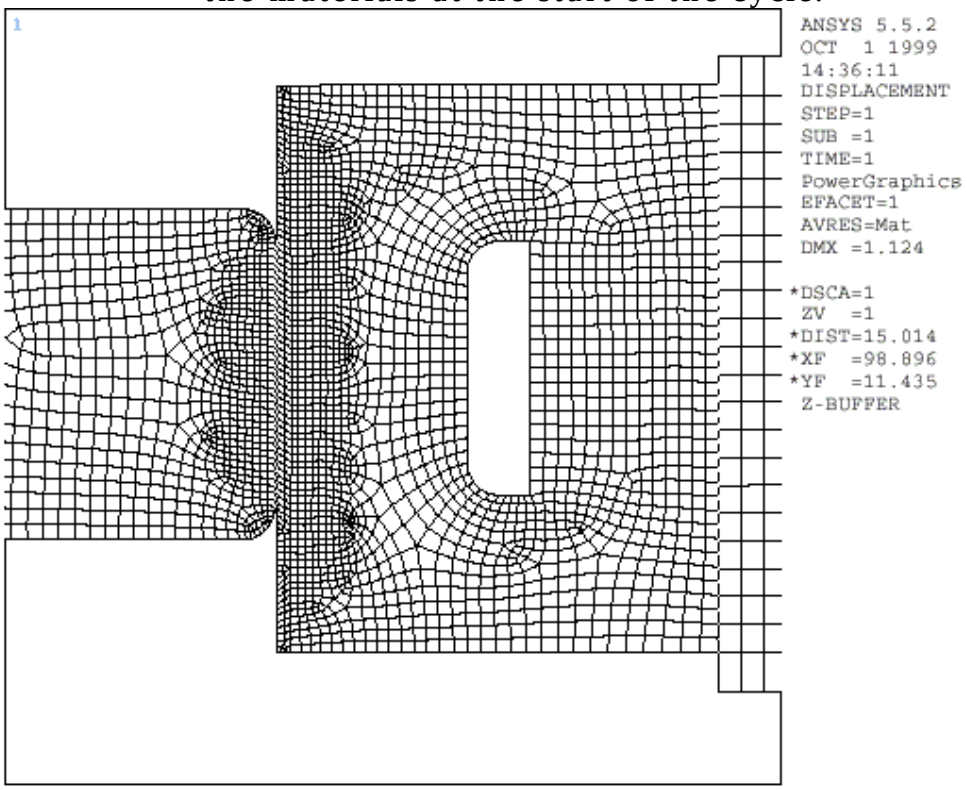

Figure 13. ANSYS model of the distorted geometry at braze temperature.

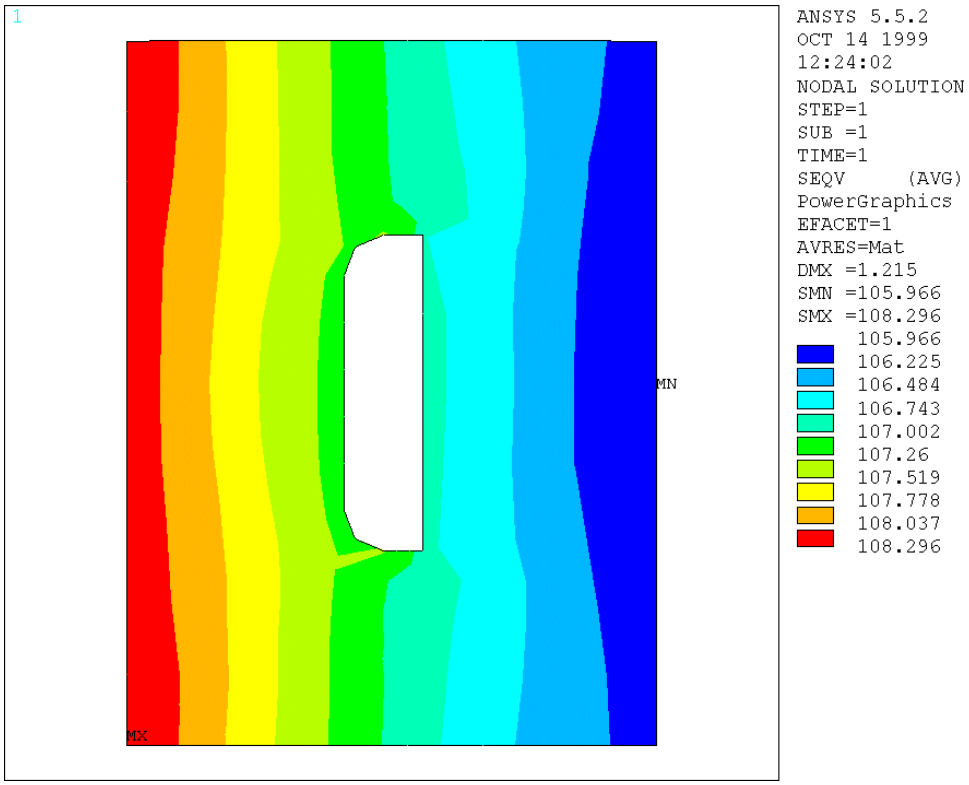

Figure 14. Von Mises stress in the stainless steel ring at brazing temperature.

4. "Bimetallic Ring" Tests

In order to test the ANSYS model, a simple experiment was undertaken. A solid stainless steel ring and a molybdenum ring were fabricated to the estimated dimensions according to the ANSYS model. The stainless steel ring was "greened" with chromium oxide and the molybdenum ring was coated with titanium nitride. The rings were assembled in a vacuum furnace and then put through a temperature cycle from room temperature to 1025°C and back, see figures 15 and 16. A simple ANSYS model was used to predict the final dimensions of the solid stainless steel ring after the cycle. After the temperature cycle the stainless ring was measured on a coordinate measuring machine (CMM). The final dimensions were close to those predicted for the stainless steel but, unexpectedly, the inner diameter of the molybdenum ring was larger after test. The initial i.d. of the ring was 8.7341" and the final i.d. was 8.7355". The molybdenum should have been operating well below the yield point even at 1000°C. The plate stock from which the ring was cut was created using pressed and sintered molybdenum powder. The most probable explanation of the slight increase in size of the ring is the densification of the material at the interface under the pressure of the stainless steel. The initial and final measurement of the stainless steel ring are given in Table 1

		I.D. "	O.D. "	Thick "
Initial Dimensions		7.4317	8.703	0.843
Final Dimensions		7.3399	8.6172	0.8502

Table 1. Dimensions of stainless ring before and after first test

When creating an FEA model of this test, the final dimensions of the stainless steel ring are very sensitive to the thermal expansion coefficients assumed for the molybdenum and stainless steel. The thermal expansion data at high temperature varies significantly from source to source. Based on average data from various sources, the initial ANSYS model predicted the final dimensions to be 0.002" larger than the actual dimensions of the test. Most of this difference can be attributed to the growth of the molybdenum ring.

A second test was done using a stainless steel ring that was 0.007" larger in diameter. This test served two purposes. First, to see if the molybdenum ring continued to change and secondly, to provide an additional data point to confirm the ANSYS analysis.

After the second test, the results were as shown in table 2. The molybdenum ring grew another 0.002” in diameter. Unfortunately the growth did not retard and appeared to be relatively constant.

	Stainless Steel		Moly
	I.D.	O.D.	ID
initial	7.4399	8.7099	8.7356
final	7.342	8.6188	8.7377

Table 2. Dimensions before and after the second ring test.

In order to further test the stability of the molybdenum ring we reused the second stainless steel ring with a 0.046” shim around it and ran it through the furnace again. This allowed us to run a third ring test without having to fabricate a new stainless steel ring.

	Stainless Steel		Moly
	I.D.	O.D.	ID
initial	7.342	8.6648	8.7377
final	7.253	8.571	8.7411

Table 3. Dimensions before and after the third ring test.

After the results of the third test confirmed that the molybdenum ring continued growing, we decided to move on to window braze tests. We had scheduled a ring test with a hollow rather than solid ring, however, ANSYS analysis showed that there were minimal differences (less than 0.001”) in the behavior of a ring with a water channel and a solid ring. By changing from a wire braze to a foil braze, we hoped to make the success of the braze less sensitive to any further growth in the molybdenum ring. Designing around a 0.001” gap at brazing temperature with 0.004” of foil in place should make the brazement more likely to succeed in these conditions. If the ring did not grow, the excess foil would be compressed and the braze would be in place, if it did grow (as much as .003” radially) the foil will still be in place in the gap, although not compressed and it should still ensure a successful braze.

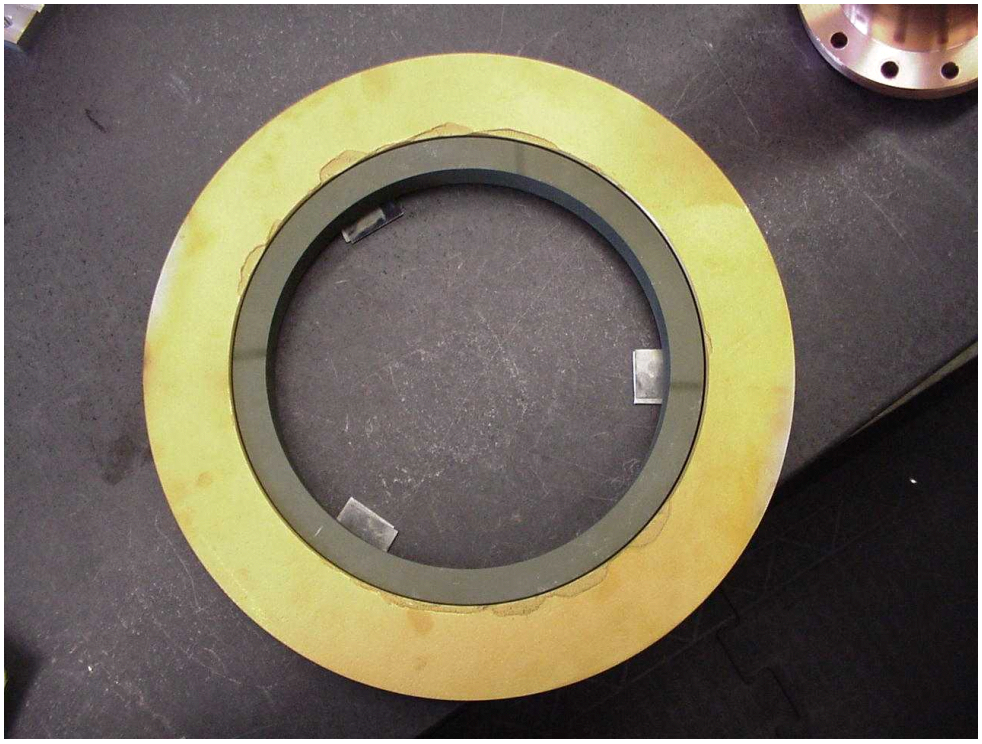

Figure 15. Molybdenum and stainless rings prior to furnace test

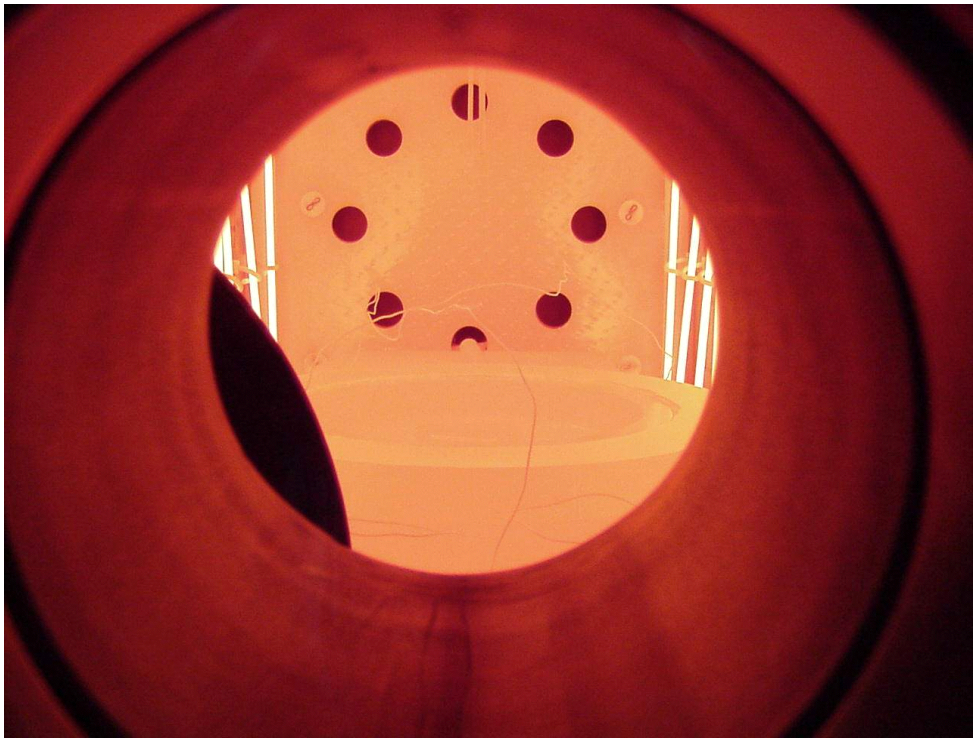

Figure 16. Stainless steel and molybdenum rings at 1025°C through the window of the furnace.

Figure 17. Hollow cooling ring parts ready for brazing.

5. Window Brazes

The brazing method and furnace profiles used were adapted from the successful SLAC PEPII window brazes. Modifications in the dimensions of the windows and brazing fixtures were made to accommodate the 700 MHz design. The temperature profile was as follows:

Temp	rate	Hours
°C	deg/min	
23		0
960	10	1.561667
960	hold, 1hr	2.561667
1025	15	2.633889
1025	hold 5 mins	2.717222
440	1	12.46722
440	hold, 10hr	22.46722
40	1	29.13389

Table 4. Braze furnace temperature set points

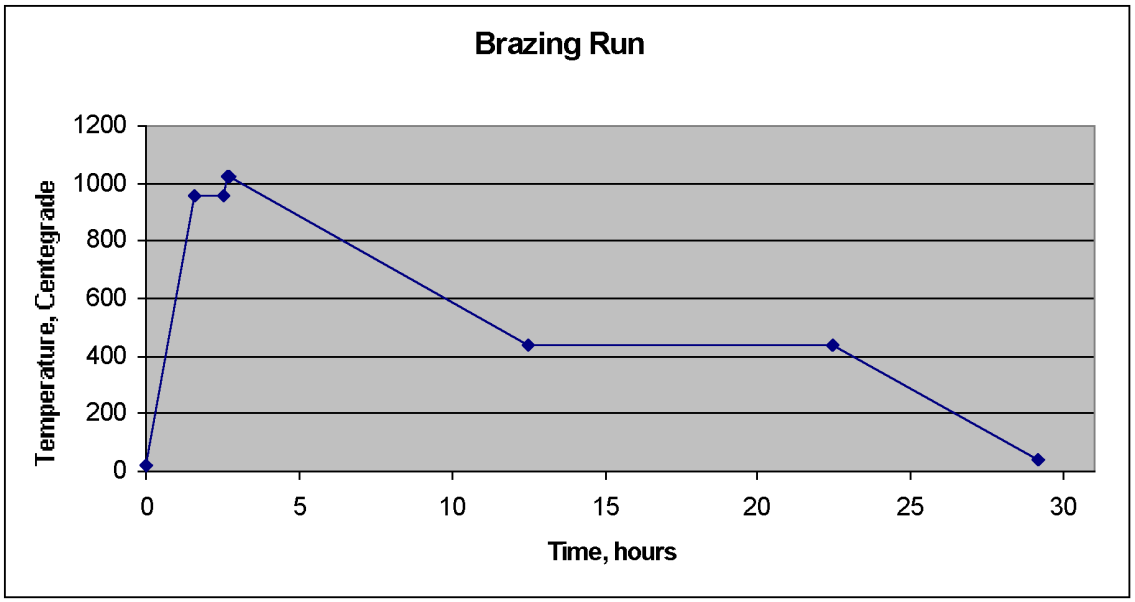

Figure 18. Braze furnace temperature profile

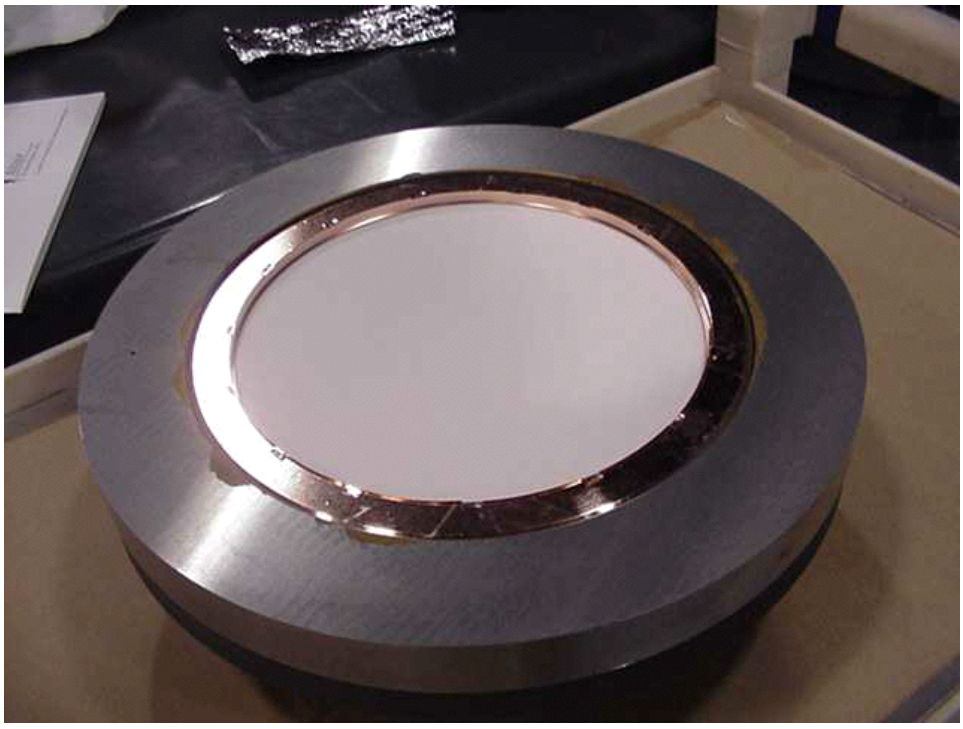

Figure 19. Fixtured window assembly ready for braze

The brazing atmosphere was a wet hydrogen atmosphere with dewpoint between -30°C and +30°C. If the braze is done in dry hydrogen atmosphere, the reducing atmosphere will remove the greening from the stainless steel, possibly causing the rings to stick together. Additionally, ceramic and copper are both cleaned

exceptionally well by a wet hydrogen environment. However, a non reducing, dry, inert atmosphere such as Argon should not remove the greening and should also be a favorable atmosphere for a brazement of this type.

Braze test 1

The first full window braze test used foil material (35-65 Cu-Au) backed up by a wire in the following configuration:

Foil braze:

2 sheets 2 mil foil.
1 ring of .040 wire.
.004" of foil, expected 1 to 3 thou gap at temperature.
i.e.: "Negative" gap at brazing temperature.

For comparison the PEPII method used:

5 .004" shims
2 rings .040
1 bead of braze paste

Given an ideal brazing gap (0.001-0.003") a foil braze and a wire braze should work equally well. However, a foil braze allows for greater versatility if the brazing conditions are less than ideal. If the brazing gap is too large due to, for example , a molybdenum ring that expands too much, the brazing wire may not flow and create a full seal. If, however, the braze is designed such that there is a 0.001-0.004" gap at brazing temperature and 0.004" of foil in the gap, the material is preplaced and does not need to flow. The excess braze material in the gap will flow out of the way as it is compressed between the alumina ring and the stainless steel ring and form the braze fillet.

Unfortunately the first brazement ended with a cracked alumina window. The braze looked smooth and uniform, but there was a crack running from the braze interface into the window. The first centimeter of he crack was relatively straight and went through the entire window. The crack continued from there in an almost complete circle along one of the surfaces. The radius of the circle corresponded almost exactly with the circle that intersected the three ball bearings that supported the weight of the alumina window. Additionally, upon removing the assembly from the

furnace, the entire weight of the brazement was resting on the three ball bearings.

Figure 20. Crack at edge of ceramic after first braze test.

There are a number of possible scenarios that could explain the failure. The hertzian contact stresses at the interface between the window and the ball bearings may have approached the yield strength for the ceramic. Rough hand calculations confirmed that this could be the case. The allowable hertzian contact stress (calculated) for this alumina was ~1200MPa, the calculated stress from the weight of the stainless steel ring and the ceramic window sitting on the three ball bearings was ~1000MPa. This was proposed to explain the circular path taken by the crack. It did not completely address the issue of crack initiation. Changing from ball bearing supports to ceramic disc supports was proposed.

The ceramic could have broken due to direct and uneven heating from the infrared radiation from the unbaffled heating elements. SLAC had some experience with this problem when baking out ceramics during the PEPII project. The fact that the Vacuum Industries furnace had a rectangular element profile could add to the uneven heating. Putting a stainless steel baffle around the braze assembly was proposed to eliminate this possibility.

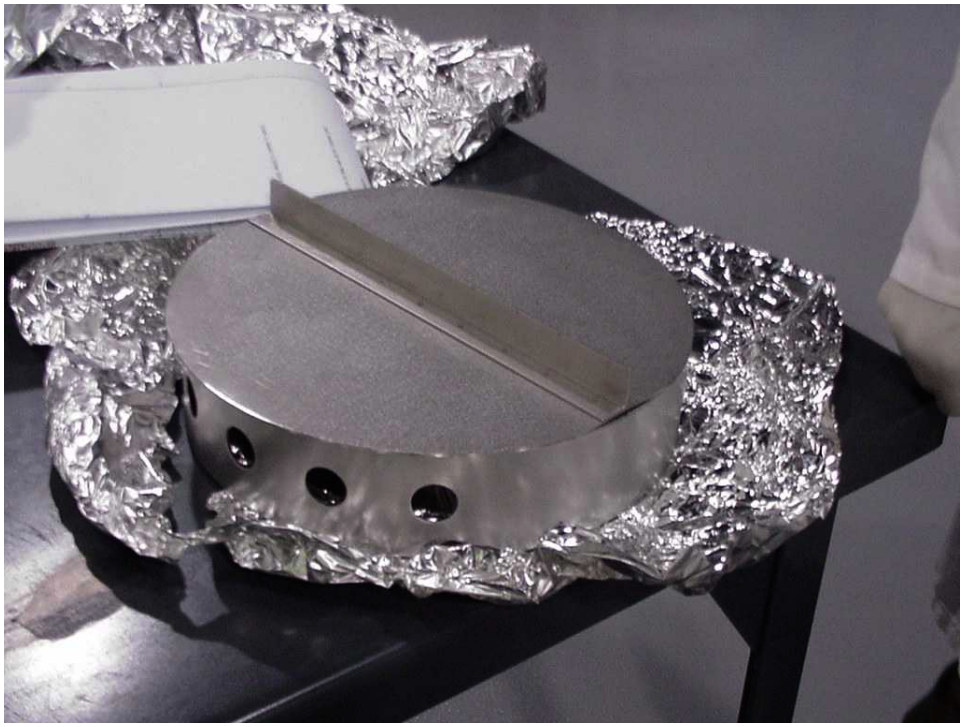

Figure 21 Sheet metal baffle used to shield braze assembly #2-5.

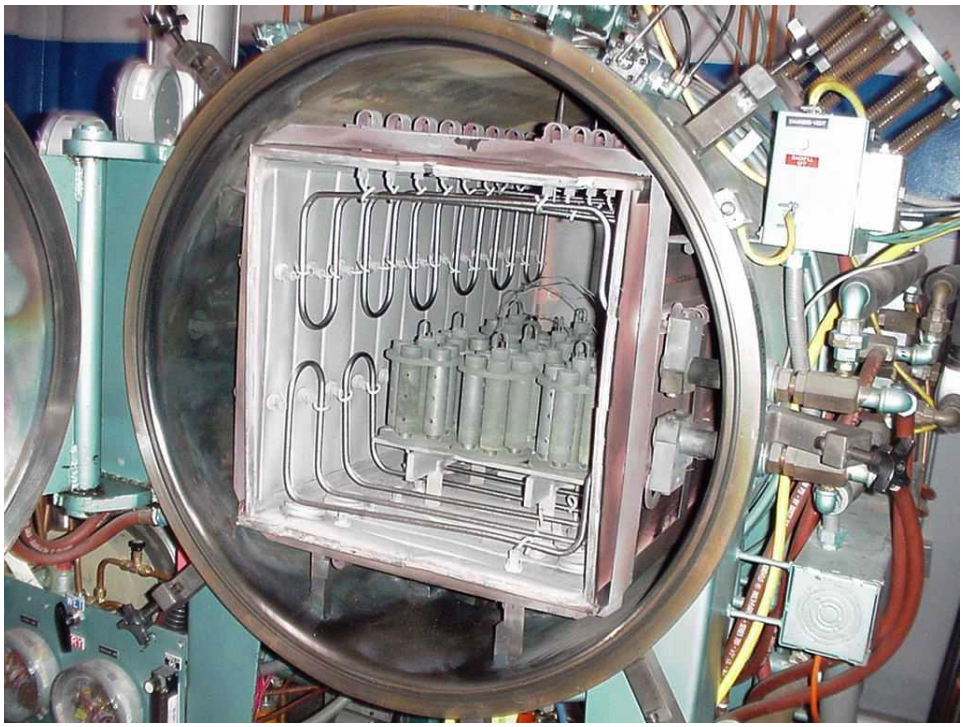

Figure 22. Square furnace with exposed heating elements.

There was some brazing material visible on the outside of the stainless steel ring from the internal water-channel joint (in this case a NiCoro alloy, Liquidus 1030C, solidus 1000C, future stainless steel

assemblies were brazed with pure copper, melting at 1083C). There was a possibility that this might have caused the stainless ring to have stuck to the molybdenum ring and as the furnace cooled to have created a tensile stress in the alumina causing it to crack. Adding a greened 0.010" stainless steel shim between the molybdenum ring and the stainless steel ring was proposed to eliminate this possibility.

There was some concern that the presence of the 0.004" foil in a 0.001-0.003" gap could cause some compressive stress that yielded the ceramic. However, any compressive stress resulting from the interference between the braze alloy and the window should be far less than the stress created by the stainless steel ring shrinking around the window during cooling. Secondly, the original SLAC braze used 1" sections of 0.004" foil in the 0.003" gap which would create corner stresses higher than any stresses created in this case. Thirdly, the temperature at which the interference would occur, is at or higher than the solidus of 35-65 Cu-Au braze alloy. This means the alloy would be soft, if not liquid when this contact occurs. However as a precaution a return to the wire braze was made for brazement #2, with the option of returning to foil brazes in the future.

There were some siginificant delays in arranging the subsequent tests because of problems with the copper plating of the stainless rings, see section 6. This should have been a straightforward process but several rings had to be stripped and replated because of blistering during the greening process. This is indicative of oxide contamination of the copper due to improper activation of the surface before plating or before restarting plating on one of the rings that was underplated at the first attempt. Further complications arose because of improper masking which allowed acid to seep under tape and caused severe etching of the stainless steel where the knife edge was to be cut. This resulted in several of the rings having to be cleaned up and thus be undersized and in one case a washer of new material had to be brazed on to replace the missing material. Fortunately all of the rings were eventually salvaged and the braze tests were able to continue.

Braze test 2

The following changes were made between braze 1 and 2:

- Disc supports instead of ball bearings for alumina window.
- Added stainless steel baffle to reduce direct infrared heating.

- Changed from foil braze to wire braze.
- Added a stainless steel shim between the OD of the stainless steel ring and the ID of the molybdenum ring.

Unfortunately due to the time and budget pressure, we did not have the luxury of changing one item at a time to pinpoint the source of trouble. For the second window brazement attempt we made all the changes at once. The second braze was successful. However, we did not know precisely which change(s) were responsible for the successful braze. The keeper ring grew slightly again during this run.

At about the same time SLAC had two PEP-II type window brazes in process using the same furnace. Both of the SLAC windows cracked in a similar manner to our first window's failure. SLAC's brazes were traditional wire brazes, with alumina discs for support and no provisions for eliminating IR shine on the window. This suggested that the heat shield was most likely the key element.

Figure 23. Window #2 as brazed.

Braze test 3

Braze #3 was a repeat of braze #2 with slightly modified shim thickness to account for the growth in the molybdenum ring. It was also successful.

Braze test 4

The foil braze was revisited for the fourth brazement. Using the same clearances as for the second and third braze, but with 0.004" of foil in the gap. The fourth braze was successful, justifying the views of the engineers that it was not responsible for the initial failure.

Braze test 5

Braze #5 was a repeat of braze#4 with a customized shim thickness to obtain the optimal clearances The growth of the molybdenum ring was significantly reduced in the last brazes, perhaps suggesting that the material was finally densified. A summary of dimensions for the first five brazes is given in the following section.

Summary of braze assembly clearances

The rule of thumb for a successful window braze using a ceramic of this size (O.D. approx. 7.375") and the molybdenum ring currently being used (I.D. approx. 8.742") is to have a total gap of 0.0250-0.0265". The gap between the alumina and the stainless steel ring should be about 0.010" and the gap between the stainless steel and molybdenum ring should be about 0.015". This rule of thumb, developed by simulation and experiment, appears to work well if the gaps are fairly well balanced in this proportion. Aiming for this total gap value should give a 0.002-0.003" gap between the alumina and stainless steel ring at the 1025C brazing temperature. Table 5 shows the dimensions of the first 5 brazes.

	#1 actual	#2 actual	#3 actual	#4 actual	#5 actual
Moly ID"	8.7411	8.7417	8.7417	8.7420	8.7407
Stainless OD"shim included	8.7100	8.7140	8.7140	8.7070	8.714
Stainless ID"	7.3945	7.3990	7.3990	7.3917	7.3990
Window D"	7.3756	7.3754	7.3754	7.3763	7.3753
Gap AS	0.0094	0.0118	0.0118	0.0077	0.0118
Gap SM	0.0155	0.0139	0.0139	0.0175	0.0133
Total Gap	0.0250	0.0257	0.0257	0.0252	0.0252
Gap at Temp	0.0017	0.0022	0.0022	0.0020	0.0020

Table 5. Dimensions of the first 5 braze assemblies

From the first ring test the inner diameter of the molybdenum ring expanded with each cycle. The ring grew 0.001-0.002" with each of the first three bimetallic ring tests. Table 6 and figure 23a show how the ring grew after each furnace run. Figure 23b shows how the ring gradually developed a slight taper in the ID. The ANSYS analysis, figure 24, predicted the peak stresses in the molybdenum ring to be on the order of 75MPa, far below the expected 160MPa yield of molybdenum at 1000C.

date	cycle#	half-height	average	OD
31-Jan	0-initial	8.7343	8.7343	12.0520
7-Feb	1-ring test	8.7354	8.7355	
6-Apr	2-ring test	8.7355	8.7355	
11-Apr	3-ring test	8.7370	8.7371	
27-Apr	4-braze 1	8.7372	8.7372	12.0339
15-May	5-braze 2	8.7407	8.7407	12.0367
18-Aug	6-braze 3	8.7405	8.7405	12.0368
26-Sep	7-braze 4	8.7407	8.7408	12.0374
31-Oct	8-braze 5	8.7412	8.7412	12.0372

Table 6 ID of molybdenum keeper ring

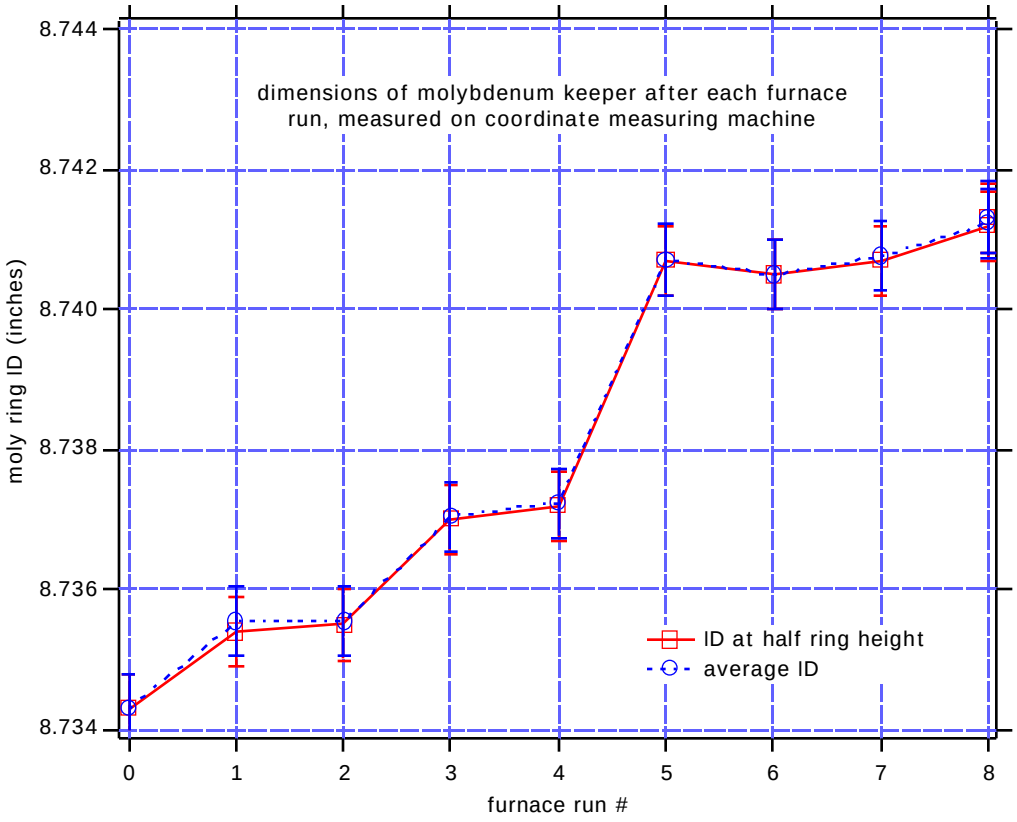

Figure 23a. ID of molybdenum keeper ring after each furnace run.

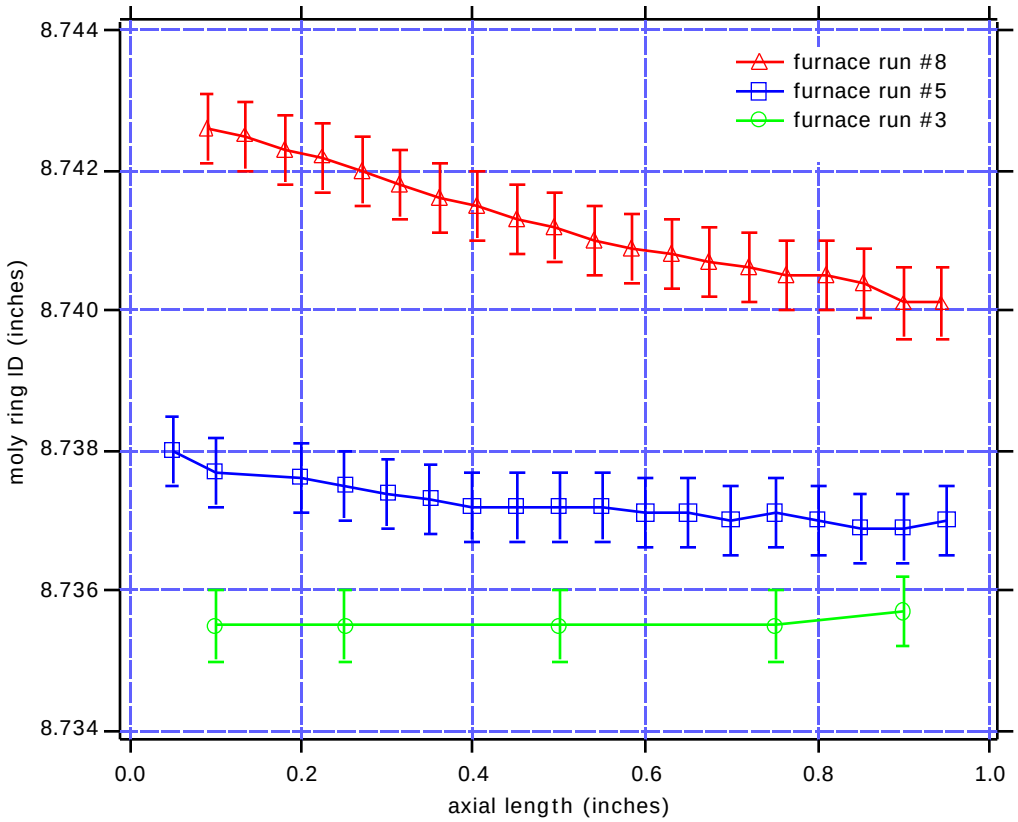

Figure 23b. Variation of ID of molybdenum ring with height.

The instability of the molybdenum ring proved to be one of the more frustrating aspects of the brazement. Over 6 furnace cycles the ring grew .008" in its inner diameter. There are several possible theories that might explain this growth:

- The ANSYS model is incorrect and the stress in molybdenum is greater than predicted in the FEA model. The stress exceeds the yield in the molybdenum and over time, as the molybdenum work hardens, the dimension stabilizes.
- The molybdenum made by a powder metallurgical process. First powder is sintered into a block and then it is rolled into plates. This rolling and densification happens mostly perpendicular to the plate. Therefore, the in-plane stress in the molybdenum may cause some densification. After a certain amount of densification the molybdenum should stabilize.
- The molybdenum used, PM molybdenum from CSM obtained through Rembar, may be in a recrystalized state, rather than stress relieved. This makes the yield strength drop quite a bit. However, literature values for the yield in RX molybdenum plate are ~150MPa at 1000C, the predicted stress in ANSYS is 75MPa.

- The solid stainless steel rings exceeded the yield point of the molybdenum, but the hollow rings did not.
- (unlikely) Something in the Argon/Vacuum furnace makes the molybdenum weaker while hydrogen furnace does not have this problem. The large growth stopped once we switched to the Hydrogen Furnace.

We believe the densification theory is the most plausible since the empirical evidence suggests that the ring is stabilizing and rough measurements of the O.D. of the ring did not show any significant growth.

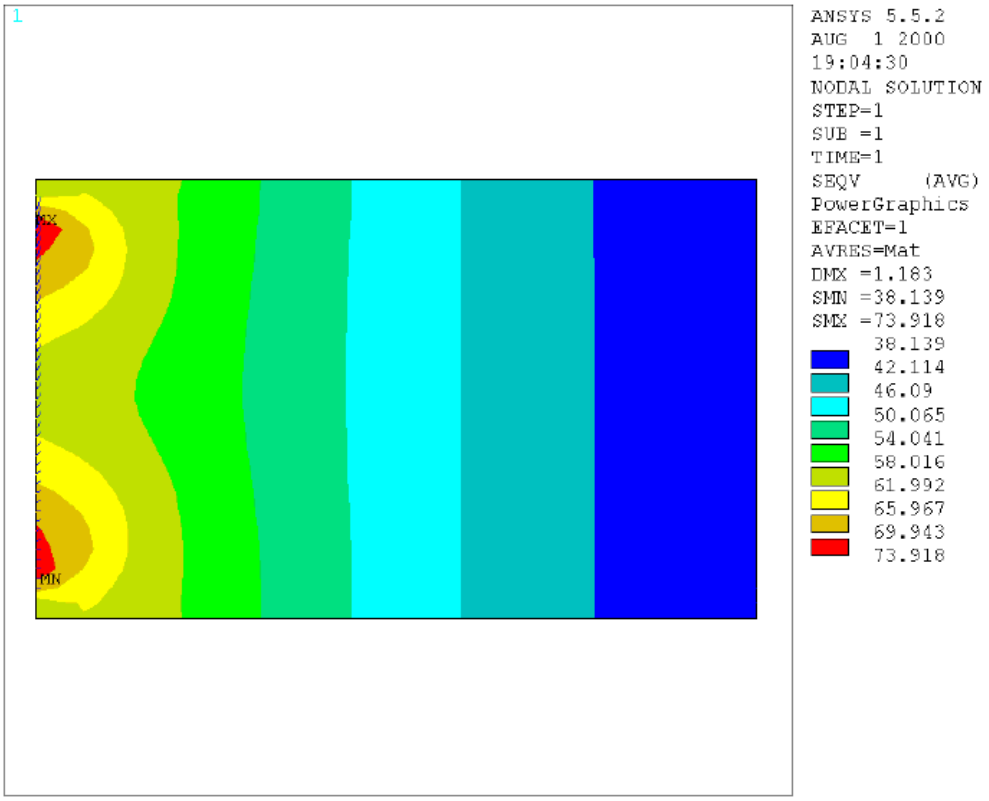

Figure 24. Stresses in the molybdenum ring at brazing temperature

6. Copper Coating

The copper coating of the stainless steel ring was done to provide a buffer layer between the stainless steel and the ceramic window. As the stainless ring contracts around the ceramic window the copper yields to relieve the high stresses generated at the corners of the ceramics. The 10 hour at 440°C hold during the furnace cycle allows the copper to creep and further relieve stresses. The original PEPII development team calculated that a 0.025" layer of copper was ideal to relieve corner stresses without losing too much of the radial compression.

The copper layer needed to be applied in an additive free bath. If there were additives in the baths, the copper layer would blister in the wet hydrogen atmosphere during green firing. The blistering may prevent a vacuum tight braze being made. Unfortunately LBNL no longer has in house copper plating facilities. All of the copper plating was done at Livermore. This prevented direct supervision of the plating process and may have contributed to some problems.

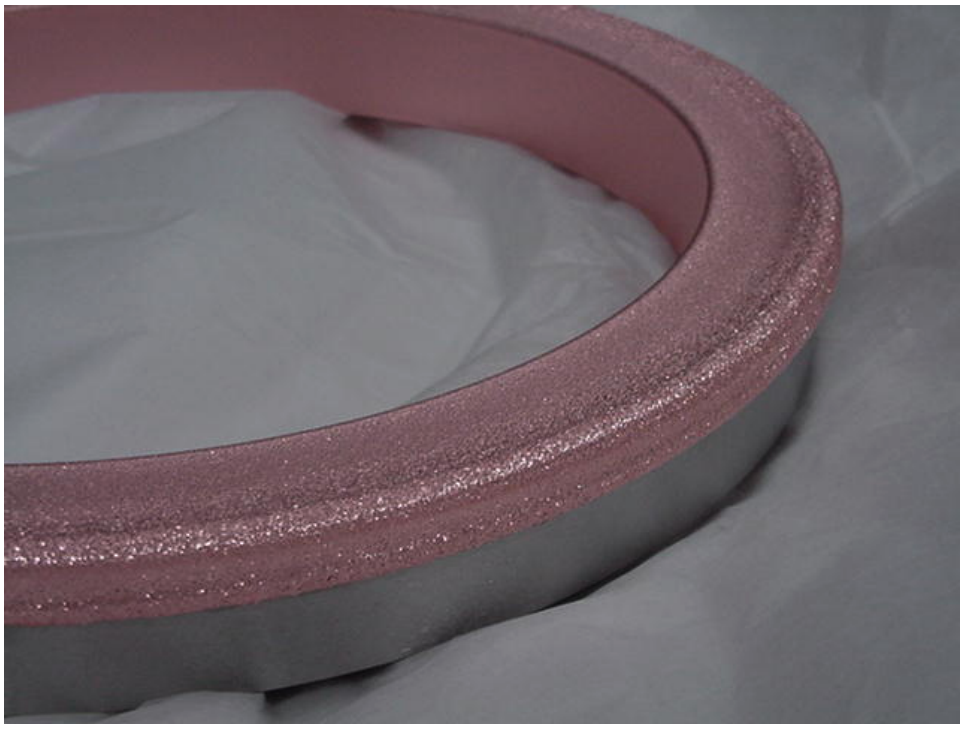

Figure 25. Copper plating on the stainless steel cooling ring.

Figure 26. Copper build-up on the corner of the cooling ring.

The additive free copper solution does not apply very smoothly, especially around corners. In order to get a 0.025” final smooth layer of copper, at least 0.010” additional machine stock must be coated over the entire piece. In order to get a 0.035 copper layer over the low spot s on the flats, we found that as much as 0.080-0.100” must be plated on the corners. Custom fixtures were made for the plating so that the rings rotated around an anode inside the ID of the ring. Even with these measures, the ring needed to stay in the plating bath for the better part of a week.

If the copper layer proved to be undersize or blistered during greening it needed to be removed completely prior to replating. It was found that if the copper layer was machined only partway off, any subsequent copper plating did not adhere well enough to avoid blistering in the greening run.

There was a recurring problem during the initial copper coating runs. When a ring was removed from the plating tank and the masking removed from the ring, etching damage in the stainless steel was noticed on 3 or 4 of the initial rings.

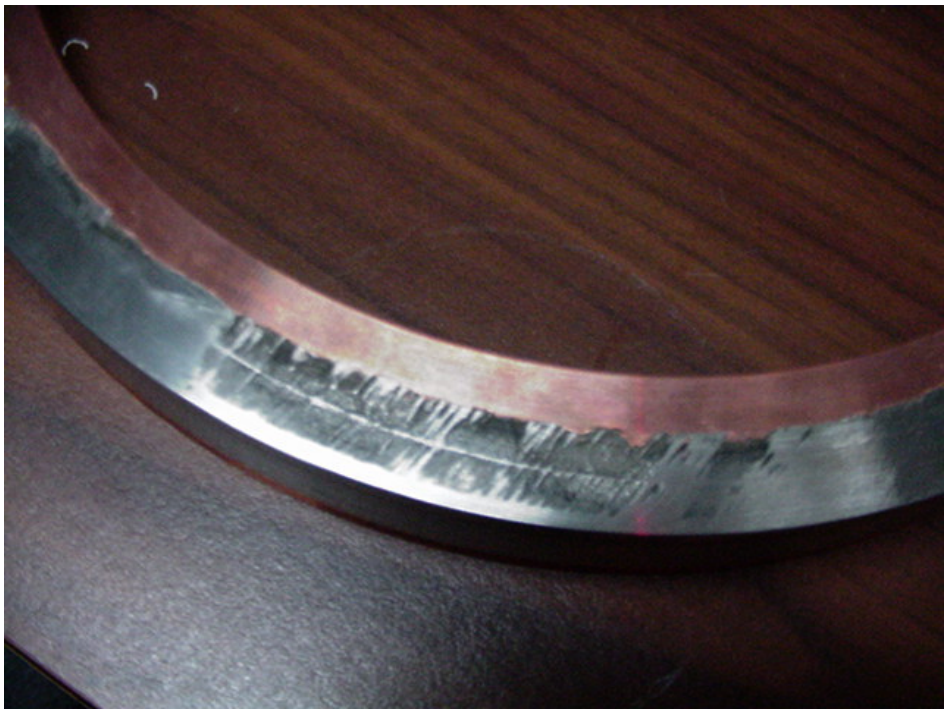

Figure 27. Etching damage on the stainless steel ring.

Figure 28. Etching damage in the stainless steel ring.

It was thought that during the initial strike, which prepared the stainless steel surface for copper plating, the hydrochloric acid in the solution may have leaked under the masking tape. The HCl solution may have sat against the stainless steel surface for the

entire coating operation, during which, it etched away the steel surface. The damage ranged from 0.020-0.080” in depth. One ring was sufficiently badly damaged that a washer of new material had to be brazed in place to effect a repair of the area where the knife edge is cut.

During subsequent coating runs, the masking tape was applied carefully to ensure that there were no large overlaps in the tape that would allow the solution to seep in. Additionally the edges of the tape were sealed with putty. These measures seemed to prevent any further problems.

Post-braze frequency measurements

After brazing the windows were once again checked in the cold-test fixture. The frequencies were consistently slightly lower than expected, although well within an acceptable range for high power testing. Some difficulty was experienced in determining the exact frequency of the best match, in part because the match of the windows was significantly better than the coax. to waveguide adapters through which the measurements were made. Simple network analyser calibration proved to be inadequate so a TRL-type calibration was used which attempted to include the adapter reflections in the calibration. This was fairly successful although in some cases there was a small discrepancy between reflection and transmission measurements using the same calibration. These residual errors may arise from small changes in the experimental set-up between measurements, drift during measurements, connector repeatability etc. The final frequency determination was taken as the average of several measurements. Shims were used to adjust the length of the iris to optimize the frequency prior to final machining. The measurement proved to be insensitive to whether the shims were placed above or below the flange.

Figure 29 shows the reflection measurement of the first (cracked) window. The match frequency is close to 700 MHz although the best measured reflection coefficient is not as low as the other windows. This is probably due to a small drift in the calibration or other measurement error. (Note that even in this case the measured match is better than -30dB which is acceptable) Window #2, the first good window, showed a slightly lower match frequency, see figure 30 The measured reflection coefficient was better than window #1, suggesting a better calibration. Despite the frequency offset the match at 700 MHz is almost -35dB (the best match is almost -47 dB). Figure 31 shows how the match frequency varies with iris thickness as spacers are inserted to raise the window or the clamping ring.

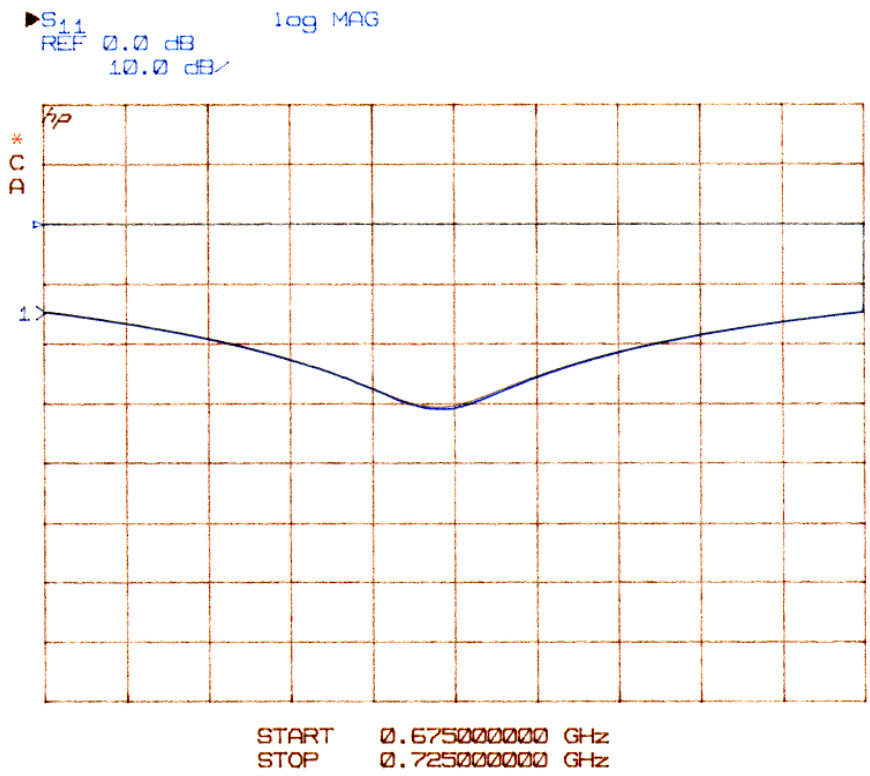

Figure 29. Window #1 (cracked) as brazed (6 shims on top)

The graph shows four data points at each height; two reflection measurements and two in transmission, along with the average. The average value seems to vary as expected with thickness, the deviation of individual data points gives an idea of the measurement uncertainty. Note that even at the full height the frequency does not quite reach the ideal value (700 MHz) expected from previous cold-test measurements. This could easily be corrected in series production bu a small change in the ceramic thickness.

Window #3 could not be cold-tested after brazing because this was the furnace run where the atmosphere dried out, the braze ran and the molybdenum buttons used to support the stainless ring became brazed to the underside.

Window #4 shows a similarly good match to window #2 at full height, also at slightly lower frequency, see figure 32.

Window #5 was measured quickly before the windows were dispatched to the machine shop for final machining. The frequency is acceptable although the broadness of the reflection curve again suggests a less than perfect calibration, see figure 33.

The frequencies of windows 2 through 5 were very consistent and these all used ceramics from the same batch. A small thickness adjustment would be appropriate for future ceramics from the same batch.

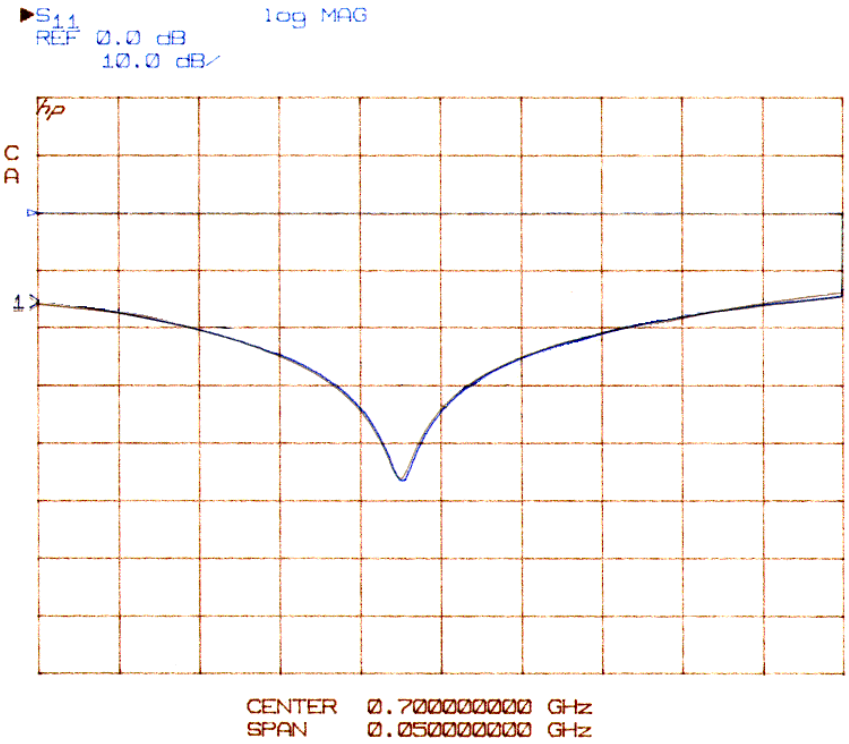

Figure 30. Window #2 as brazed (5 spacers underneath)

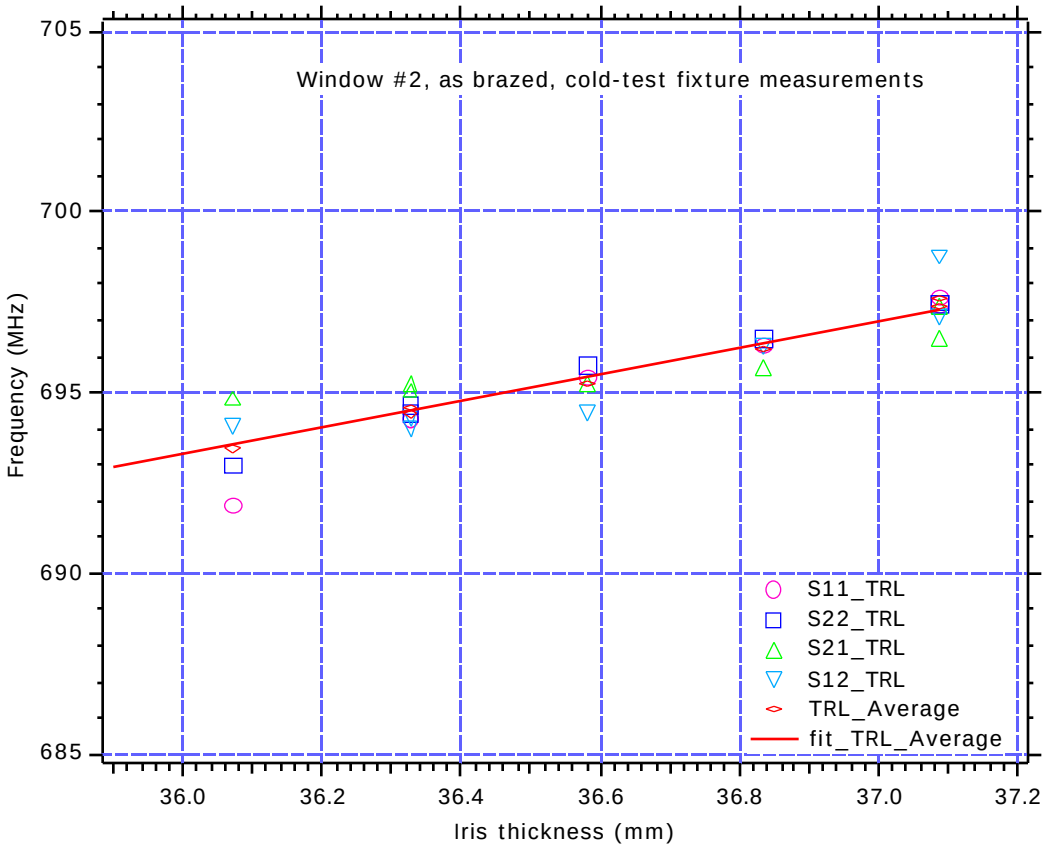

Figure 31. Window #2, frequency dependence on iris thickness

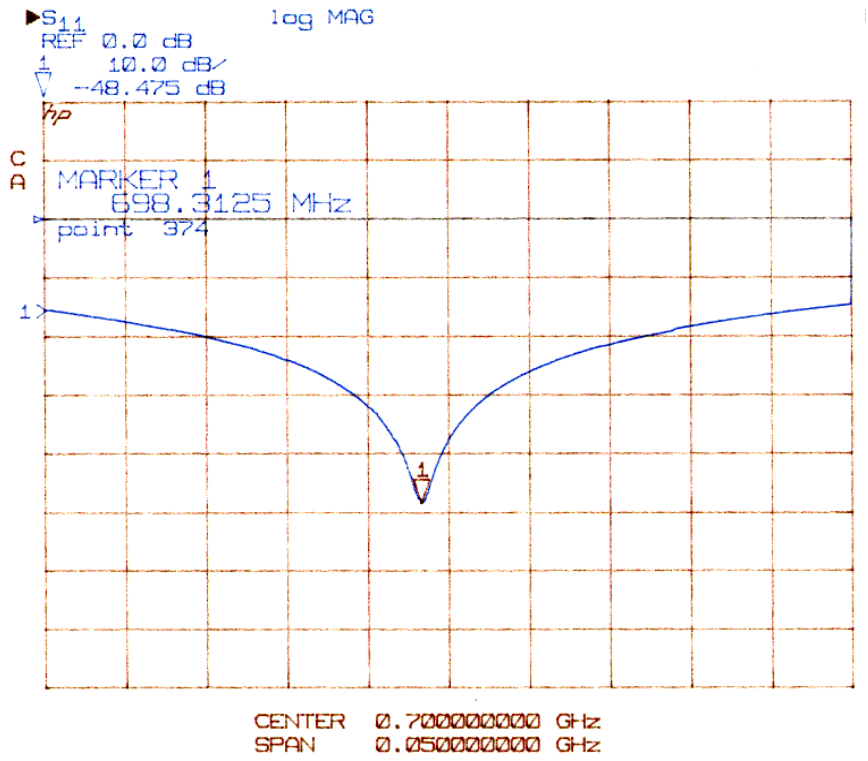

Figure 32. Window#4 as brazed (8 shims underneath)

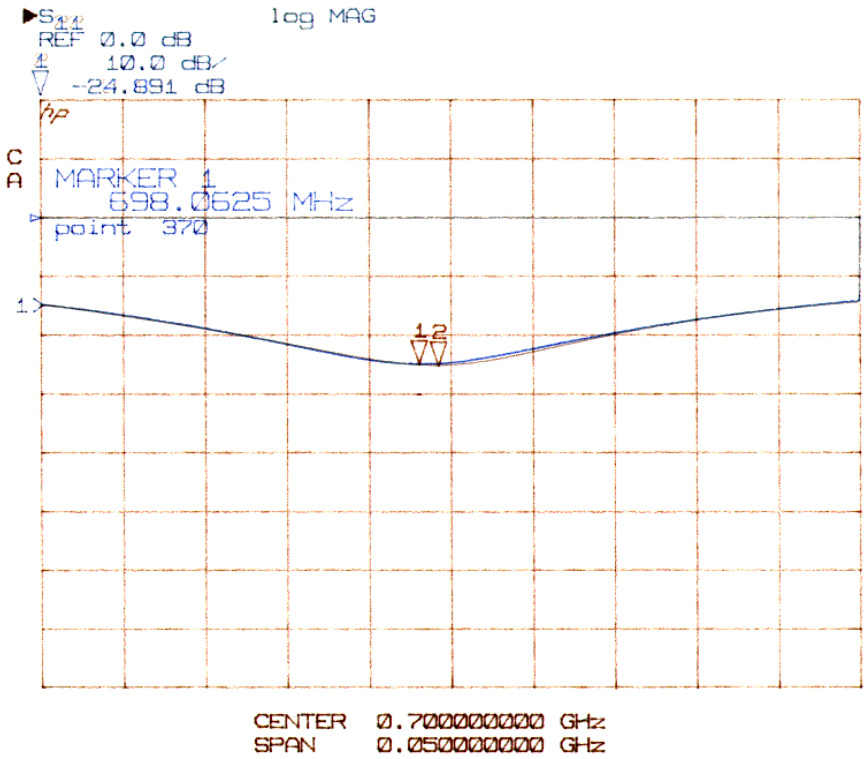

Figure 33. Window #5 as brazed (10 shims on top)

8. Final machining

After brazing and leak checking the windows are machined to final dimensions. At this point they are considered clean assemblies and are handled only with lint-free gloves and only alcohol is used as a cutting fluid/coolant. The lathe was cleaned thoroughly and a new, cleaned, six-jaw chuck was used to hold the windows. RF measurements of the brazed window assemblies showed that the flanges should be kept at the maximum thickness to minimize the frequency offset so all four windows were cut to the same thickness. The knife edge was cut first, using the cooling channel holes as a reference to gauge the center of the cooling ring. Finally the copper layer on the air side surface was faced off to provide the final thickness. In three cases the dimensions were chosen to center the ceramic in the cooling ring. In once case it was not possible to achieve this because the cooling ring had been etched on one side and the knife edge surface had to be cut slightly deeper. However the match frequency is quite insensitive to this dimension.

9. Final frequency measuremnts

The first window to be cut to final size, window #4 was fitted to the real spool box with the customized waveguide spacer and torqued down using a spare RF gasket, see figure 34. This was the first frequency measurement of the final configuration. The match was good (over -47 dB) and the frequency was 697 MHz (-0.4%). The match at 700 MHz was about -33 dB, which should be acceptable for high power testing. The other windows were also tested before shipment . Window #1, the cracked window was also tested in the spool to add a further data point. Ironically it had the closest frequency and best match at 700 MHz. The results are summarized in table 7. The average frequency from all the reflection measurements of the first 5 windows is 696.625 MHz, which is 3.375 MHz below the desired operating frequency. This would require a 0.169 mm (0.0066") reduction in the ceramic thickness to correct for future windows and a further 0.702mm (0.0276") to tune the window up to 714 MHz for NLC. This would make the final thicknesses 11.31 mm (0.4454") and 10.78 mm (0.4244") respectively.

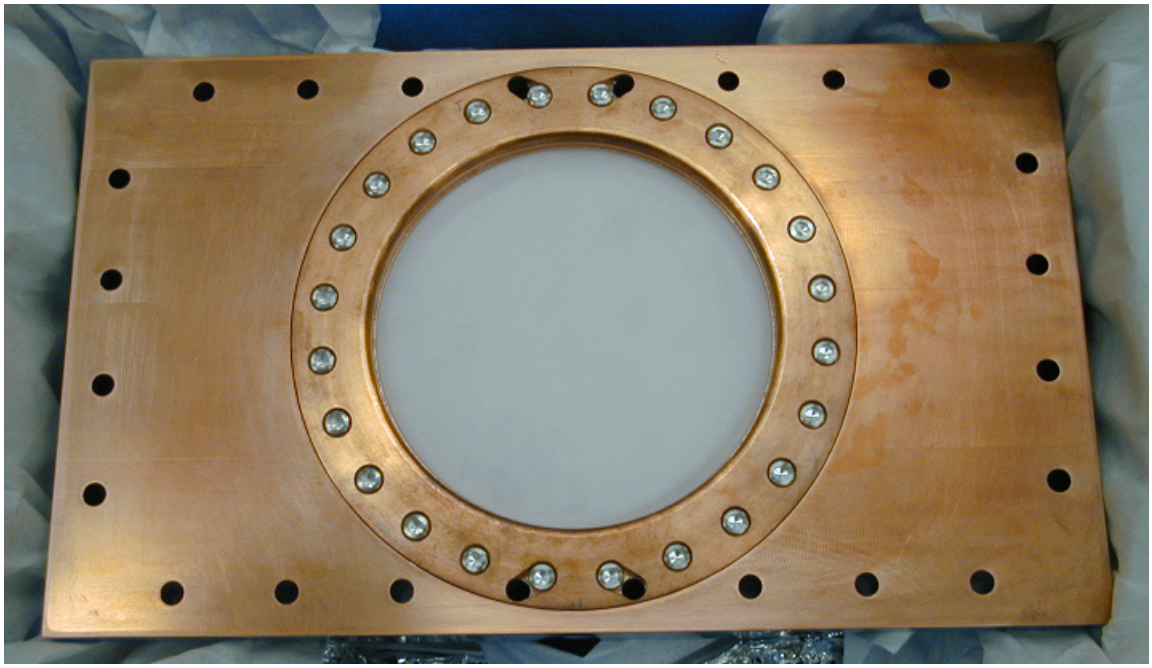

Figure 34. Finished window in spool for final frequency check.

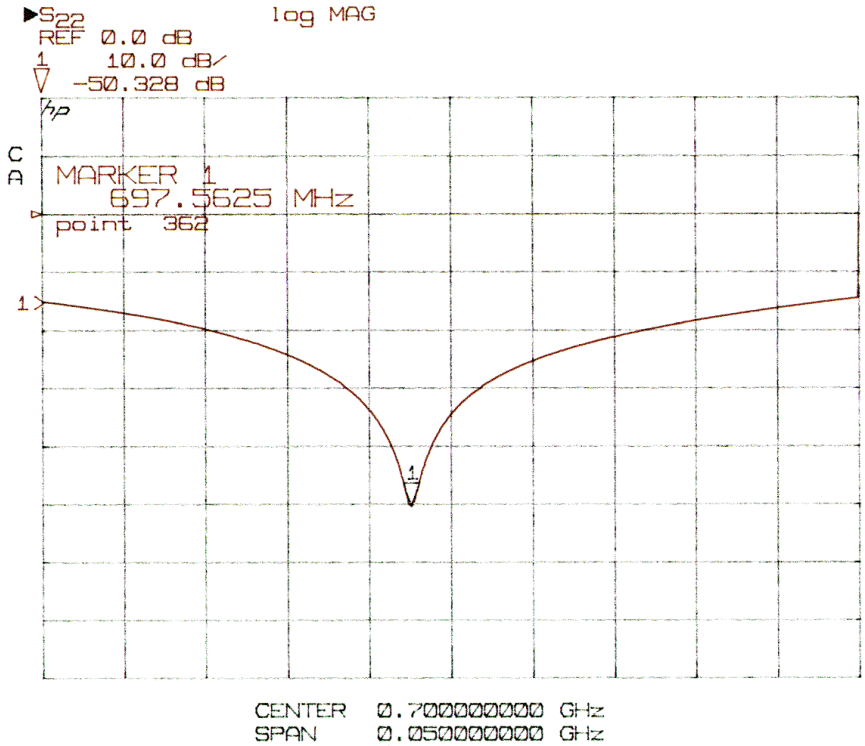

Figure 35. Window #1 (cracked) final frequency measurement in spool

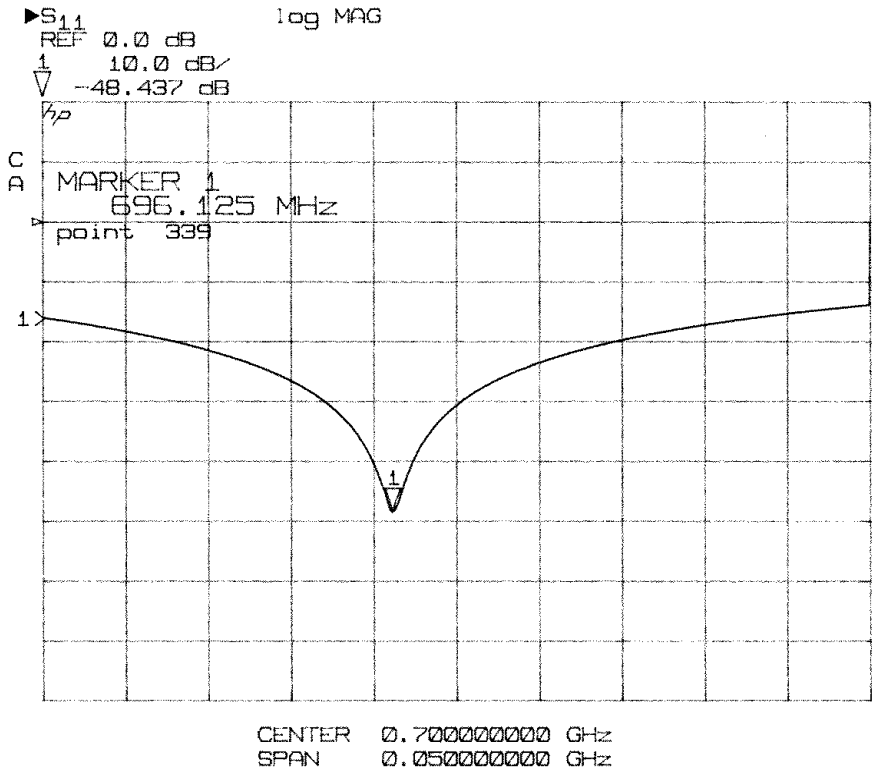

Figure 36. Window #2, final frequency measurement in spool

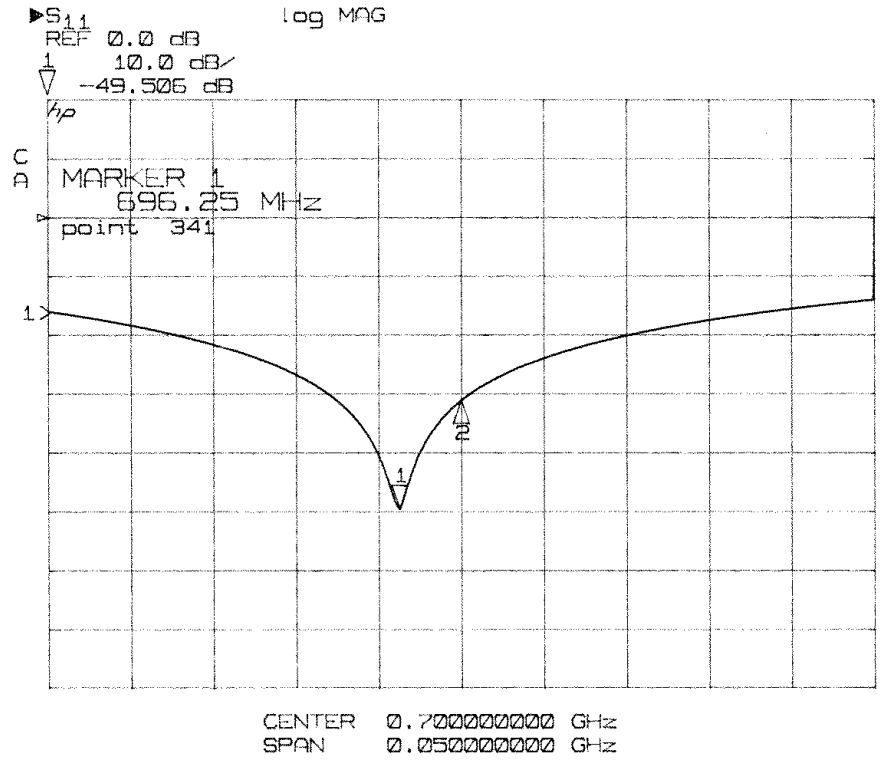

Figure 37. Window #3, final frequency measurement in spool

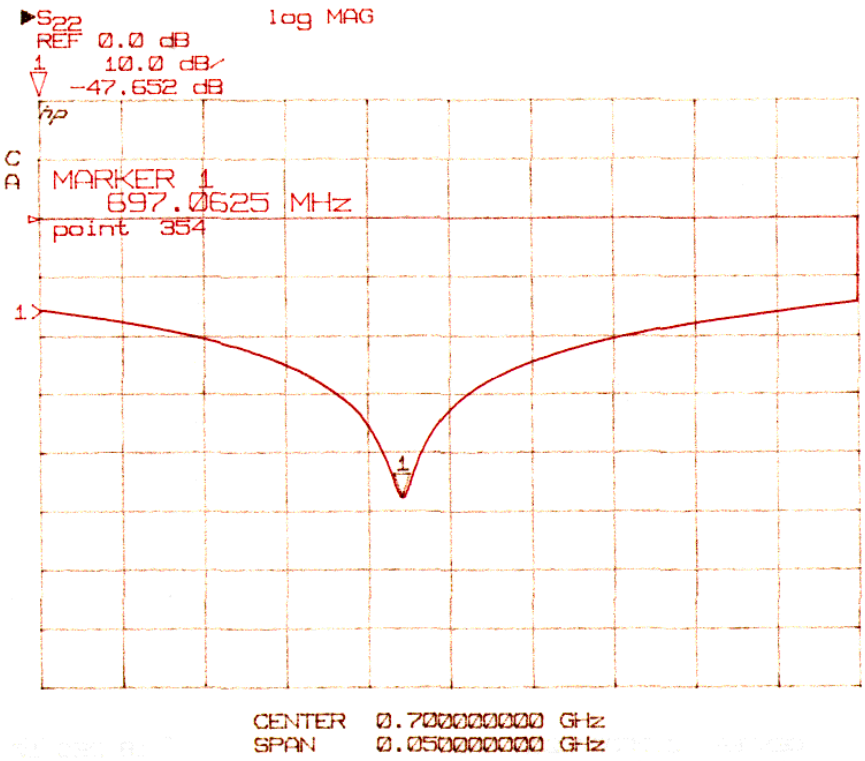

Figure 38. Window #4, final frequency measurement in spool

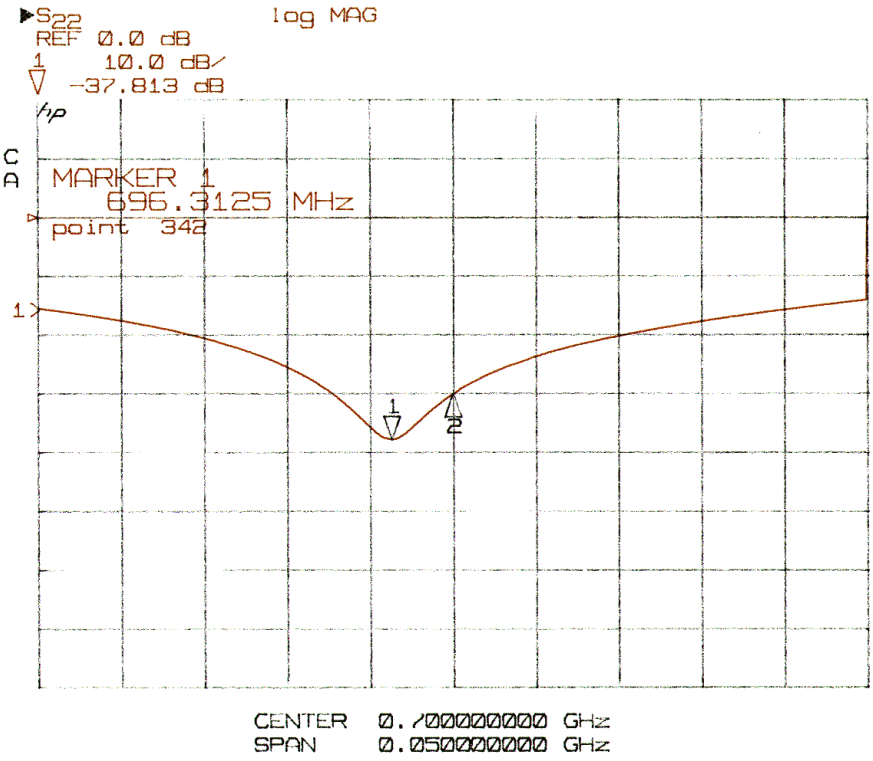

Figure 39. Window #5, final frequency measurement in spool

window#	final freq S_{11} (MHz)	match S_{11} dB	S_{11}@ 700 MHz, dB	final freq S_{22} (MHz)	match S_{22} dB	S_{22}@ 700 MHz, dB
1	697.8125	-43.148	-35	697.5625	-50.368	-34
2	696.1250	-48.437	-30.618	695.8125	-53.781	-29.777
3	696.2500	-49.506	-31.086	696.0000	-43.326	-30.16
4	n.m.	n.m.	n.m.	697.0625	-47.652	-33
5	696.6875	-35.23	-30.34	696.3125	-37.813	-30.061
average	696.7188	-44.0803	-31.7610	696.5500	-46.5880	-31.3996
average of all meas.:	696.6250	-45.4734	-31.5602			

Table 7. Summary of final frequency measurements.
(n.m.= not measured)

10. TiN coating

A thin coating of titanuim nitride (TiN) is recommended for the vacuum surface of the window to inhibit multipactoring [3]. For PEP-II this was applied by sputtering from a titanium target in a partial atmosphere of nitrogen following a "recipie" developed over many years of klystron window development. The rate of deposition was determined by experimentation with coupons which were analyzed by Rutherford backscattering (RBS). This proved to be the most accurate way to determine the amount of Ti deposited. Earlier attempts to measure the thickness from electrical properties proved to be very inaccurate because the resitance of the coating varies greatly depending on small changes in composition and history, such as exposure to air, baking etc. The optimum coating for the PEP-II windows was $6x10^{15}$ atoms/cm^2 which is thick enough to prevent multipactor but thin enough to provide low RF losses. We recommend the same for the 700 MHz windows. The coating is barely visible to the eye, but a slight gold tinge may be noticable. The coating should be uniform across the ceramic (although slightly thicker at the outer extremities may be permissible), and should extend over the braze fillet onto the copper of the cooling ring. Typically the knife edge is shielded during coating.

11. Assembly procedure

This window design is unusual in that the ceramic is strongly coupled to the mounting flange. This provides the strength to resist thermal expansion from RF heating but also means that care must be taken during assembly to avoid putting unwanted stresses into the ceramic. The coupling box and clamping ring are designed so that the forces required to make the knife edge seal are aligned opposite each other on the window flange. The pressure point on the top of the flange is on the bevelled corner at the same radius as the knife edge. This should prevent unwanted torquing of the window.

The window is designed to use copper "conflat" type gaskets with the OD of a standard 10" flange gasket. Standard gaskets could be used for leak checking purposes but a flared "serf seal" gasket should be used for RF testing. This prevents RF currents from passing through the knife edges and exposed stainless steel surfaces. Note that the first coupling box provided came from the vendor with knife edge dimensions and gasket counterbore that were out of specifications. We decided not to attempt to rework this box but instead provided slightly modified gaskets. Future boxes should be inspected to ensure compliance with the drawings so that standard gaskets can be used.

A new, clean, scratch free gasket should be used each time and be handled only with lint-free gloves. Small shims may be helpful in centering the window in the iris since the final flange OD is slightly smaller than a standard conflat flange. A new slant-spring RF seal should be inserted into the groove in the clamping ring. Silver plated bolts are supplied to prevent galling. The heads are cut down because of the limited depth of the clamping ring. A good unworn hex key should be used to avoid the risk of rounding the bolt heads.

We recommend tightening the window flange using incremental torque settings working around and across the window in a star pattern, see figure 40 We used five intermediate torque values (40, 60, 90, 120, 150 inch-lbs) and then repeating the patttern ten times at full torque (180 inch-lbs / 15 ft-lbs). This maintains even pressure aound the flange during tightening and ensures all bolts are fully torqued at the end. Tests showed that the gasket continues to compress and the bolts continue to turn through at least eight or nine cycles, see figure 41.

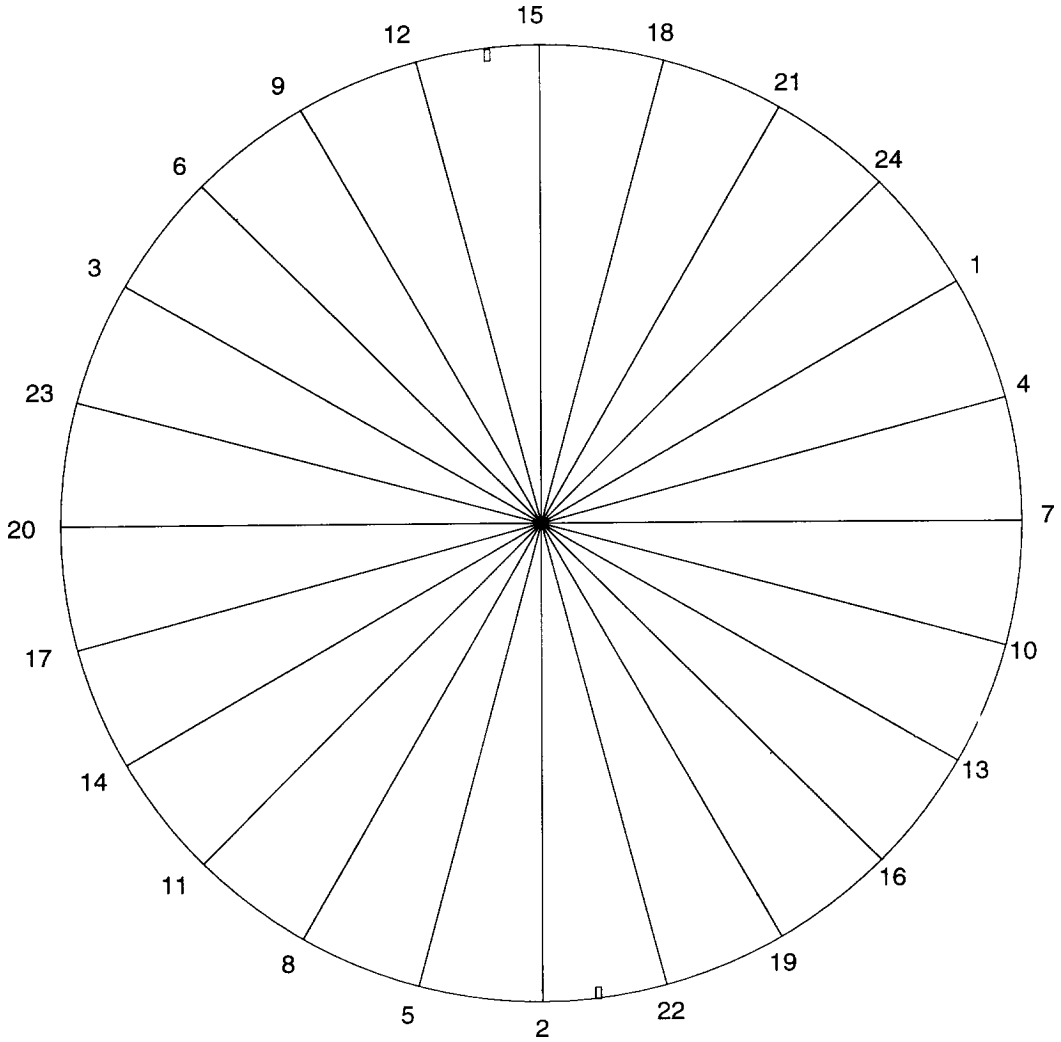

Figure 40. Recommended bolt torquing sequence

The first four prototype windows came out slightly low in frequency, possibly because of a slight change in dielectric properties in the second batch of ceramics. This meant the window flanges were left as long as possible to keep the match frequency as close as possible to the 700 MHz operating frequency. (If the windows had come out high they could have been tuned downwards by shortening the flange). In practice the small deflection of the claming ring with the full thickness flange prevents the mating waveguide from sitting completely flush with the coupling box. This was alieviated by using a waveguide spacer with a small (0.040") undercut to accomodate the raised portion of the window. For series production a small reduction in the ceramic thickness would eliminate this problem by raising the natural match frequency of the windows.

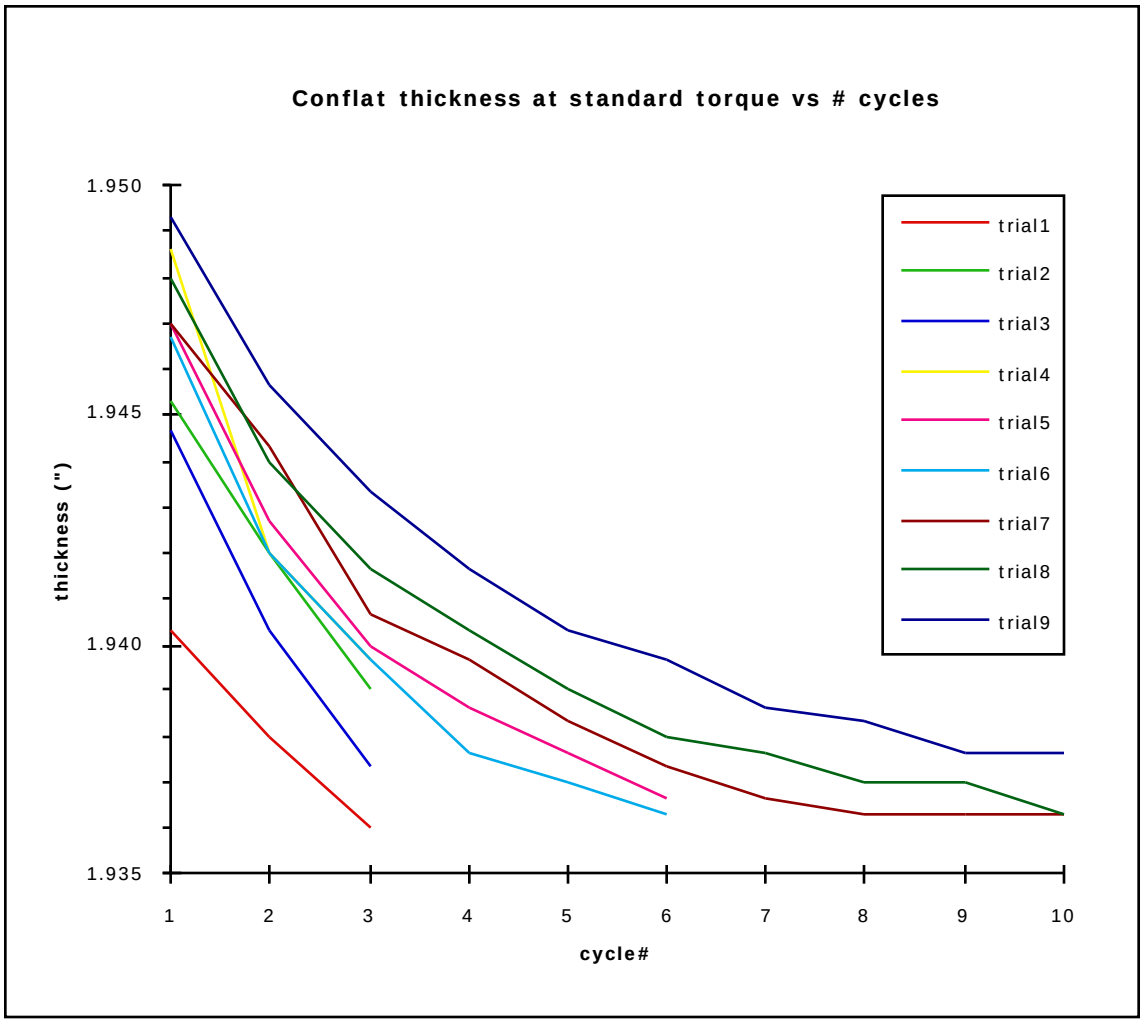

Figure 41. Compression of flange pair with repeated torquing

12. Bakeout

Bakeout is very important for the safe and rapid comissioning of the windows [3]. The windows and coupler assembly should be baked to at least 150°C and held there long enough for all the adsorbed gas to be pumped away (typically about 8 hours for PEP-II). Combined with a slow ramp up and down in temperature this process typically took two to three days. The PEP-II window assembly was baked in a large panel oven. The new window assembly will be baked using portable heater jackets, see figure 42. Early PEP-II windows that were not baked or were baked to less than 150°C proved difficult or impossible to condition to full power. Windows that were properly coated and baked conditioned quickly to full power with no glowing and very little outgassing.

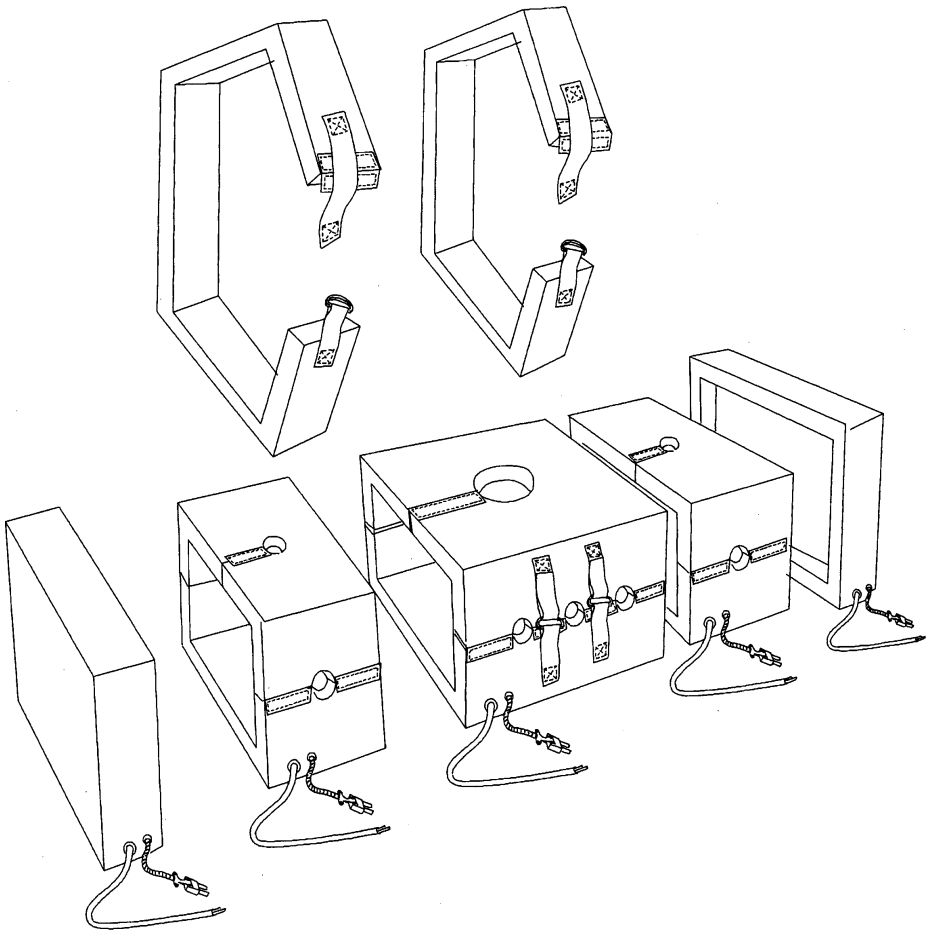

Figure 42. Portable bakeout jackets

13. Conditioning and testing

The windows should condition quickly if successful coating and bakeout have been achieved. The window test apparatus should have fast interlocks triggering on visible light (arcs or glowing), preferably on both sides of the ceramic since it is too thick to transmit an appreciable amount of light, and on vacuum pressure, which should ideally be kept below $1x10^{-8}$ Torr. If the windows are tested in transmission into a matched load then a fast reflected power interlock is useful as it is often the first indicator of an arc. A single window may be tested into a short, in which case the reflected power interlock cannot be used (unless it is to diagnose unexpected losses in the system indicating a breakdown). Note that when testing into a short the electric fields in the standing wave may be up to twice as high as the transmission test, depending on the distance from the window to the short, and therefore the window Ohmic and dielectric

losses may be up to four times greater. An infra-red temperature monitoring device looking at the center of the window is extremely valuable. If the test stand is to run unattended at any point this should be interlocked to trip off the RF in case of thermal runaway. Note that the time constant for the window to heat up and cool down is of the order of 20 to 30 minutes, so changes should be made slowly, especially when pushing to high power. The temperature rise with power should be approximately linear (~0.06°C/kW). Any significant departure from this behavior, such as a sharp upward turn in the temperature vs power characteristic, may indicate the onset of multipactoring. If the temperature coefficient is much higher than expected then multipactoring may be ocurring even at low power or there may be excessive ohmic losses from the coating. One way to check this is to back-fill the chamber with dry nitrogen and run with RF at modest power. If the losses are Ohmic the temperature rise should be about the same. If there is electronic activity in vacuum it should not take place in the gas filled chamber. Interestingly at least one PEP-II prototype window ran cooler in vacuum after this test than before, perhaps indicating the exposure to nitrogen had improved the coating properties.

A well baked and coated window should be able to be comissioned using CW power with relatively few trips. The power should be increased slowly and smoothly while monitoring the vacuum pressure for any activity and observing the window for signs of glowing (a TV camera is useful for this since it can detect very small amounts of light). Occasionally incandescent spots may be seen due to dust or contaminants on the window surface. These may process away or not, but didn't seem to be a problem for PEP-II. If glowing, outgassing or frequent arc trips persist then the window may have to be pulse conditioned. This is usually a sign that the coating is not working properly or the surface has become contaminated. In this case the RF should be applied in short pulses, raising the peak power with low duty factor until full voltage can be sustained across the window. The pulse length can then be extended to increase the average power. This process should be sufficient to clean up mildly contaminated windows, but if the coating is defective it may be impossible to process up to full power. If pulse processing is used and glowing is evident then multipactoring is happening on each pulse, terminated only when the RF is removed. This can help to clean the surface but may also cause additional heating of the ceramic and must be used with care. The power extracted from the RF by multipactoring electrons may easily be enough to break the window. If arcing and outgassing are evident in the test box but

don't appear to be related to window activity it may be helpful to TiN coat the box and spool(s) (with windows safely removed of course). This can be done with a commercial titanium sublimation source (heated ball or filament) and is far less critical in thickness and composition than the window coating.

Scaling from PEP-II performance the window should operate comfortably at 300-350 kW throughput into a matched load. This is the expected operating range of the NLC damping ring cavity windows that are intended to share this design. This may also be sufficient for LEDA operation. At this power level the temperature rise (ΔT) from the center of the window to the cooling ring should be about 20°C. However there is assumed to be a substantial safety factor in the design. Some PEP-II prototypes have run as high as 100°C ΔT (in fault conditions) without failing. This would scale to approximately 67 °C ΔT for the 700 MHz window, or roughly 1 MW throughput. Note that the PEP-II windows have never been operated routinely at such elevated temperatures. Also no good window has ever been tested to destruction so the absolute limit is not well known and will surely vary with individual coating, brazing and material variations. Hopefully this limit will be investigated one way or another during high-power testing at LANL.

14. Interesting future developments

Vacuum furnace foil braze

There appears to be no reason that the brazement could not be done in a conventional furnace under a partial pressure of argon. Although the “cleaning” properties of hydrogen would not be available, we have not had a problem with Cu-Au foil brazes failing due to cleanliness issues in this kind of furnace at LBNL. One possible concern is the behavior of the alumina window when heated in a “dry” atmosphere. Lower purity Al_2O_3 can react badly at high temperatures in a non reducing atmosphere, however the alumina windows we use are of very high purity. Additionally, during Brazement #3 at Altair, the hydrogen bubbler failed halfway into the temperature ramp. This essentially meant that the braze occurred in a dry hydrogen environment. No ill affects were noted, other than the fact that the greening disappeared on the stainless steel, causing the braze material to flow excessively and braze the molybdenum spacers to the stainless steel ring. This presumably would not occur

in a vacuum furnace as neither the vacuum nor the Argon would remove the greening.

Diffusion Bonds Between copper and alumina.

Copper oxide and Al_2O_3 have a fairly similar lattice parameter spacing. There is a fair amount of literature (although it is not easily available) that supports the diffusion bonding of copper to alumina. This might suggest that running the furnace cycle without any braze allow and slightly negative clearance between the alumina and the cooling ring could produce a vacuum tight bond.

Diffusion bond or direct braze between stainless steel and alumina.

Given the difficulties experienced with the pure copper plating it would be advantageous to eliminate the copper coating of the stainless steel ring. There is some literature to support that Al_2O_3 can be diffusion bonded directly to stainless steel. This however would eliminate the copper buffer layer between the ceramic and steel which is thought to be necessary to relax the local stresses on the corners of the ceramic. This could be investigated experimentally.

Alternatively instead of copper plating the ID of the brazement, a copper sleeve of 0.050" copper plate, could be brazed to the ID of the ring. Since the coefficient of thermal expansion of copper is similar to that of stainless, the braze would not require any special jigging. NiCoro filler metal (Bau-3, 1000C solidus, 1030C liquidus) could be used to braze the plate to the ID of the stainless. With careful assembly the water channel braze and the ID copper braze could all be done with NiCoro in the same furnace run.

Alternative materials

Traditionally high power RF windows have usually been made of high purity alumina or occasionally beryllia. Alternative materials such as aluminum nitride may have favorable properties from the standpoint of RF losses and thermal conductivity as well as manufacturability. Aluminum nitride might be brazed without metallization using an active braze alloy. The window design could be adapted to the different dielectric constant of alternative materials by adjusting the proportions.

15. Conclusions

We have successfully made four high-power RF windows which will be tested at 700 MHz as part of the LEDA project at Los Alamos. The fabrication method closely follows that of the PEP-II RF windows developed at SLAC and which have proven reliable in operation. The RF design of the window was developed using numerical simulations in MAFIA and verified by cold-test measurements. Measurements of the finished windows in the real fixture showed good agreement with expectations. The small residual frequency offset observed could easily be tuned out in subsequent production. The unexpected loss of the first brazement in the furnace was a disappointment and caused us to delay production of the subsequent prototypes while it was investigated and modifications were made to the process. It is now believed that the failure was due to the use of an unshielded furnace with exposed electrical heater elements. The use of a simple heat shield appears to have eliminated this problem. The success of the four subsequent brazes, two using wires and two using foils suggests that this process can be used with confidence in the future.

We eagerly await the results of high power testing of these prototypes.

16. References

[1] "High-Power RF Window and Coupler Development for the PEP-II B Factory", M. Neubauer et. al., Proc. PAC 95, Dallas, TX, SLAC PUB 95-6894, LBNL-37250.

[2] "High-Power RF Window Design for the PEP-II B Factory", M. Neubauer et. al, Proc EPAC 94, SLAC PUB-6553, LBL-35920.

[3] "High-Power Testing of PEP-II RF Cavity Windows", M. Neubauer et. al, Proc EPAC 96, Sitges, Barcelona, Spain, PEP-II AP 96.04, SLAc PUB 7209.

Appendices

A Pre-Brazement Fabrication Checklist
B Brazing Spec
C Notes on Brazing and furnace runs
D Cost estimate
E Sample drawings

Appendix A: Pre-Brazement Fabrication Checklist:

Molybdenum Ring

- Rough machine ring
- Stress relieve to at least 1100℃ (above the highest brazing temperature)
- Finish grind ring
- Coat ID of molybdenum ring with TiN
- Molybdenum is now ready for brazement

Ceramic Windows

- Grind ceramics to diameter and thickness for specified frequency
- Radius the corners of the window
- Metalize the OD of the window, nickel.
- Ceramic ready for braze

Stainless steel rings:

- Water channel Braze:
  - Rough machine sub-assemblies
  - Stress relieve to at least 1100C (above the highest brazing temperature)
  - Finish Machine to tight brazing tolerance
  - Braze two subassemblies in vacuum furnace, Cu wire at 1083℃.
  - Leak check the water channel
- Post-braze machine the ring to pre-copper coating dimensions
- Copper coat the ring with plenty of machine stock
- Machine the copper coated ring to final pre-braze dimensions.
- Green fire the ring in wet hydrogen atmosphere.
- Ring is now ready to braze

Appendix B: Brazing specification:

Materials

- Copper coated stainless steel to Metalized Al_2O_3, braze is copper to nickel.

Filler Metal 65-35 Cu-Au, 0.002” braze foil, 0.040” wire, solidus: 990°C, liquidus: 1010°C

Braze Geometry:

- Faying surfaces are concentric faces. ID of SS ring and OD of ceramic disc.

Cleaning: UHV clean Parts and brazing material before assembly

Assembly

- Assemble SS ring inside molybdenum ring
- Assemble ceramic disc inside ssring,
- Assemble brazing foil and wire
- Reference assembly drawing #25J0116

Braze foil preparation

- Braze foil should be cut to exact length as the SS ring I.D. Ends should be square cut and butted together.
- Wire should be cut to exact length and butted. It should be loaded inside the foil ring, ref Drawing #25J0116

Brazing: Hydrogen Furnace, wet hydrogen atmosphere, dewpoint between -30 deg C and +30 degC

Temp	rate	Hours
C	deg/min	
23		0
960	10	1.561667
960	hold, 1hr	2.561667
1025	15	2.633889
1025	hold 5 mins	2.717222
440	1	12.46722
440	hold, 10hr	22.46722
40	1	29.13389

Table 8. Braze furnace temperature set points

Inspection and pressure checking

- Visually inspect part for obvious contamination or poor filler flow
- Inspect for gaps in braze
- Helium leak check parts across window

Appendix C: Notes on brazing and furnace runs:

- The stainless steel rings were brazed together using OFHC copper filler metal, melts at 1083°C.

- The first stainless steel ring and some subsequent repairs were made using the NiCoro alloy, Liquidus 1030°C, solidus 1000°C. When these rings were put through further furnace cycles, some braze material re-wetted and occasionally flowed. With the exception of the first brazing run, this did not present a problem. During the first run, some NiCoro filler metal flowed from the stainless steel ring to the molybdenum and left some residue on the ID of the molybdenum ring. This residue could have allowed the stainless steel ring to bond to the molybdenum. The filler metal residue was removed with an acidic solution.

- Greening was done in a wet hydrogen atmosphere at Alpha Braze in Freemont, CA.
  - The coating time was left up to the vendor , the only specs were:
    - The rings were green coming out (a visible coating)
    - The temperature was kept as low as possible (1000-1010°C) and did not exceed 1025°C (the final brazing temperature)

- The TiN coating on the Molybdenum was done by BryCoat in Florida.
  - Again the spec was for a visible coating of TiN on the ID of the molybdenum ring.
  - There were no other specifications.

Appendix D: Cost estimate

Prototyping is an inherently expensive activity and bringing a new RF window to production readiness can be an unpredictable and time consuming process. We attempted to minimize the cost and risk of this development by basing the process on a well-proven design developed (at great expense) for PEP-II. Apart from the failure of the first braze test, which is now thought to have been caused by lack of shielding in the furnace, the basic process has validated by four consecutive successful brazes. Significant costs and delays were incurred due to problems in the copper plating process which should have been straightforward. The largest costs were labor for engineering and production coordination overhead which would be amortized over a much larger number of windows in volume production. An upper estimate of the window cost can be made by taking the cost of this contract and dividing by the four successful windows. The basic contract (with extension) totalled $120k, while direct procurements from LANL and additional manpower and services at LBNL (provided from NLC project funds) probably doubled that figure. Thus the actual cost of the first four windows was of the order of $60k each (though it could have been $48k if the first braze had been good). This is not an unreasonable amount for prototypes but contains a large amount of start-up and development costs that should not recur in volume production

Table 9 contains a "success oriented" bottoms up cost evaluation based on continuing production using the same procedures, assuming an average labor rate of $75 / hr. Not included are engineering and production oversight, which would be amortized over the total number of windows produced. Note that spool cost may be reduced by eliminating unnecessary features, such as spare viewports.

material/operation	hours	$labor	$M&S
"prodek" plate stock ($275 for 2 sets rings)			137.50
metallized ceramic ($1895 for 5)			379.00
Braze material, wire ($759/130" 6 windows)			126.50
Braze material, foil ($1036.5/150", 3 windows)			345.50
1. Measure ceramic and keeper ring dimensions	3	225.00	
2. Burn rings for cooling ring parts	1	75.00	
3. Rough machine inner/outer rings	3	225.00	
4. Stress relieve roughed rings.	1.5	112.50	
5. Finish machine inner/outer ring set.	8	600.00	
6. UHV clean prior to brazing.	1.5	112.50	
7. FurnaceBraze cooling rings.	1	75.00	
(4.0 hours for 4 rings)			
8. Machine prior to plating.	4	300.00	
9. Copper plate ring.	8	600.00	
10. Machine plated ring.	10	750.00	
11. UHV clean prior to greening.	1.5	112.50	
12. Green fire ring. (per run)			600.00
13. UHV clean prior to brazing.	1.5	112.50	
14. Prepare for brazing ceramic into ring.	4	300.00	
15. Furnace Braze ceramic into ring.			2675.00
16. Finish machine knife edge, tap pipe	8	600.00	
thread, finish height and recut bevel.			
17. UHV clean after machining.	1.5	112.50	
subtotals		4312.50	4263.50
window subtotal		8576.00	
19. Manufacture water fittings (8 hours for 6)	2.7	202.50	
20. Manufacture waveguide spool (est.)			11000.00
21. Clamping ring manufacture (125 hours for 2)	62.5	4687.50	
plating (8 hours for 2)	4	300.00	
cleaning (3 hours for 2)	1.5	112.50	
clamp ring subtotal		5100.00	
22. SERF gasket	3	225.00	
23. modify clamping screws (4.5 hrs/100)	1.125	84.38	
subtotal		9924.38	15263.5
total		25187.88	

Table 9 manufacturing cost breakdown estimate for volume production (excluding engineering overhead), assuming $75 / hr.

Appendix E: Drawing package

25J0004_RF_Window_assy-integratn
25J0013_ceramic_window_dimensions
25j0022_prefire_ring_dimensions
25J0033_inner-outer_ring_machining
25J0042_window_cooling_connection
25J0056_window adapter_spool_sht_1-of-3
25J0056_window adapter_spool_sht_2-of-3
25J0056_window adapter_spool_sht_3-of-3
25J0066_window_clmp_ ring_mach_1-of-2
25J0066_window_clmp_ ring_mach_2-of-2
25J0074_moly_backup_ring_sht_1-of-2
25J0074_moly_backup_ring_sht_2of-2
25J0084_serf_vac_seal
25J0092_hx_skt_hd_screw_mod
25J0104_rf_window_fab_sht_1-of-4
25J0104_rf_window_fab_sht_2-of-4
25J0104_rf_window_fab_sht_3-of-4
25J0104_rf_window_fab_sht_4-of-4
25J0116_window_brazement_fixturing
25J0122_window_brazing_support
25J0132_window_braze_support_shim
25J0143_serf_seal_form_tool
25j0154_window_brazement-spacer_shim
25J0166_window_brazing-IR_baffle
25J0176_rf_spacer_mod